Inflammopharmacology (2025) 33:845–864
https://doi.org/10.1007/s10787-024-01603-y

Inflammopharmacology

ORIGINAL ARTICLE

Anorexigenic and anti-inflammatory signaling pathways of semaglutide via the microbiota–gut––brain axis in obese mice

Rodrigo Soares da Silva[1,2] · Igor Henrique Rodrigues de Paiva[1,2] · Ingrid Prata Mendonça[1,2] · José Roberto Botelho de Souza[3] · Norma Lucena-Silva[4] · Christina Alves Peixoto[1]

Received: 23 October 2024 / Accepted: 5 November 2024 / Published online: 25 November 2024

Abstract

Our study focused on a mouse model of obesity induced by a high-fat diet (HFD). We administered Semaglutide intraperitoneally (Ozempic ®—0.05 mg/Kg—translational dose) every seven days for six weeks. HFD-fed mice had higher blood glucose, lipid profile, and insulin resistance. Moreover, mice fed HFD showed high gut levels of TLR4, NF-kB, TNF-α, IL-1β, and nitrotyrosine and low levels of occludin, indicating intestinal inflammation and permeability, culminating in higher serum levels of IL-1β and LPS. Treatment with semaglutide counteracted the dyslipidemia and insulin resistance, reducing gut and serum inflammatory markers. Structural changes in gut microbiome were determined by 16S rRNA sequencing. Semaglutide reduced the relative abundance of Firmicutes and augmented that of Bacteroidetes. Meanwhile, semaglutide dramatically changed the overall composition and promoted the growth of acetate-producing bacteria (Bacteroides acidifaciens and Blautia coccoides), increasing hypothalamic acetate levels. Semaglutide intervention increased the number of hypothalamic GLP-1R+ neurons that mediate endogenous action on feeding and energy. In addition, semaglutide treatment reversed the hypothalamic neuroinflammation HDF-induced decreasing TLR4/MyD88/NF-κB signaling and JNK and AMPK levels, improving the hypothalamic insulin resistance. Also, semaglutide modulated the intestinal microbiota, promoting the growth of acetate-producing bacteria, inducing high levels of hypothalamic acetate, and increasing GPR43+ /POMC+ neurons. In the ARC, acetate activated the GPR43 and its downstream PI3K-Akt pathway, which activates POMC neurons by repressing the FoxO-1. Thus, among the multifactorial effectors of hypothalamic energy homeostasis, possibly higher levels of acetate derived from the intestinal microbiota contribute to reducing food intake.

Keywords Obesity · GLP1 agonist · Gut–brain axis · Semaglutide · Acetate

Introduction

Obesity is a worldwide public health problem, with approximately 1.5 billion people overweight or affected by obesity. Obesity has been well-characterized as a close risk factor for developing a range of metabolic diseases, including type 2 diabetes mellitus (DM2), atherosclerosis, cardiovascular disease (CVD), and steatotic liver disease associated with metabolic dysfunction (MASLD) (Loh et al. 2019; Song and Zhang 2022). There is increasing evidence that the gut–brain axis plays an essential role in multiple aspects of physiology, including regulating feeding and appetite, glucose homeostasis, and gut motility (Richards et al. 2021). The composition of gut microbiota is regulated by factors such as genes, diet, and medication therapy (Jandhyala et al. 2015; Hasan and Yang 2019; Qin et al. 2022). Several metabolic diseases, including obesity and diabetes are associated with altered

✉ Christina Alves Peixoto
christina.peixoto@fiocruz.br

1 Laboratory of Ultrastructure, Laboratório de Ultraestrutura, Aggeu Magalhães Institute (IAM), FIOCRUZ, Av. Moraes Rego S/N, Recife, PE CEP 50670-420, Brazil

2 Postgraduate Program in Biological Sciences/Center of Biosciences, Federal University of Pernambuco (UFPE), Recife, PE, Brazil

3 Department of Zoology, Federal University of Pernambuco, Recife, PE, Brazil

4 Laboratory of Immunogenetics, Aggeu Magalhães Institute (IAM), Recife, PE, Brazil

gut microbiota (dysbiosis) (Clemente et al. 2012; Sonnenburg and Bäckhed 2016; Bliesner et al. 2022). Anti-diabetic medications can alter the gut microbiota and, otherwise, the gut microbiota also can alter the therapeutic efficacy (De La Serre et al. 2010; Wu et al. 2017; Wang et al. 2018; Lee et al. 2018; Hupa-Breier et al. 2021). Therefore, it is crucial to understand the impact of anti-diabetic medications on the gut–brain axis.

Gut microbiota produces short-chain fatty acids (SCFAs) in the large intestine through anaerobic fermentation of indigestible polysaccharides found in dietary fiber (Silva et al. 2020a). Among the SCFAs produced by the gut microbiota, acetate, propionate, and butyrate have important functions in intestinal homeostasis, activating G protein-coupled receptors (GPCRs) 41 and 43, which are abundantly expressed in gastrointestinal tract cells, where they modulate the intestinal permeability by increasing tight junction proteins such as zonula occludens and occludin (Ang and Ding 2016). SCFAs can increase the expression of leptin and insulin, secreted from adipose and pancreatic cells, and the secretion of Peptide YY(PYY) and Glucagon-like peptide-1 (GLP-1) by colonic epithelial cells through GPR41 and GPR43 activation. Those peripherally derived signals can activate/inhibit hypothalamic neurons to regulate feeding behavior and long-term energy homeostasis (Xiao et al. 2020). SCFAs can also enter the systemic circulation and reach the CNS, where they modulate the structure and function of glial cells and stimulate the generation of new neurons by regulating the levels of neurotrophic factors through the activation of GPR41 and 43 (Razazan et al. 2021; Fock and Parnova 2023). SCFAs also have anti-inflammatory effects on the brain, as demonstrated in neuropathological mouse models (Ang and Ding 2016; Razazan et al. 2021).

The hypothalamic arcuate nucleus (ARC) is a specific hypothalamus area that regulates energy metabolism, especially in food intake (Sohn 2015; Anandhakrishnan and Korbonits 2016). At a cellular level, the ARC consists of two distinct neural populations and functionally antagonistic, one subset of neurons proopiomelanocortin (POMC) (anorexigenic) and the other the orexigenic neuropeptide Y (NPY)/agouti-related peptide (AgRP) neurons (orexigenic) (Baldini and Phelan 2019; Jones et al. 2019). POMC neurons in the ARC are nutrient and energy responsive and express several receptors, such as the insulin receptor (INSR), Glucagon-like peptide-1 receptor (GLP-1R) and, the leptin receptor (Lepr) (Secher et al. 2014). When exposed to a consumption of a high-fat/ high carbohydrate diet the regulating anorexigenic mechanisms are impaired by the misregulation of the insulin and insulin-like growth factor, FoxO and Sirtuins signaling pathways (Liu and Zheng 2021; Du and Zheng 2021a; Drucker 2022).

GLP-1 is an incretin anorexigenic hormone secreted from intestinal L cells in response to nutrient intake and incretin hormone-based therapies, such as liraglutide and semaglutide, have emerged as important agents for body weight (BW) loss and DM2 management (Wilding et al. 2021). GLP-1 receptor agonists inhibit food intake via action at GLP-1 receptors in several CNS areas, mainly the brainstem and hypothalamus, responsible for food intake regulation. In addition, GLP-1 receptor agonists have peripheral actions, slowing gastrointestinal transit and enhancing insulin secretion from pancreatic beta cells in response to glucose (Perdomo et al. 2023), but the delay gastric emptying on weight loss seems to be minimal, thus its mechanisms appear to affect energy intake without energy expenditure (Singh et al. 2022a). Besides GLP-1 improves intestinal barrier functions by stimulating crypt cell fission, reduces pro-inflammatory cytokines produced by immune cells, and modulates the composition of the gut microbiota (May et al. 2019).

Semaglutide is a long-acting glucagon-like peptide 1 receptor agonist (GLP-1 RA) approved by regulatory agencies in the USA and Europe for the treatment of type 2 diabetes mellitus (T2DM) and obesity or overweight (Lexchin and Mintzes 2023). Preclinical studies suggest that semaglutide accesses the brainstem, septal nucleus, and hypothalamus, mobilizing the neural circuits involved in the modulation of food intake through brain GLP-1Rs. Semaglutide does not cross the blood–brain barrier (BBB) but reaches the brain through the circumventricular organs and regions adjacent to the ventricles (Gabery et al. 2020a; Martins et al. 2023). It reduces BW through direct interaction with different populations of GLP-1R, besides affecting the activity of neural pathways (Gabery et al. 2020b). Clinical trials have demonstrated that semaglutide has superior efficacy compared to other antidiabetic medications in decreasing the weight, as well as reducing the rate of cardiovascular death, myocardial infarction, and stroke (Singh et al. 2022a; Chao et al. 2023).

The modulation of hypothalamic energy homeostasis is complex and multifactorial. Although several studies have demonstrated that semaglutide has a direct action on hypothalamic GLP-1R and neural pathways involved in food intake, reward, and energy expenditure (Gabery et al. 2020b), its action on the gut microbiota–brain axis is little known. This study is the first to show that semaglutide reversed the HDF-induced hypothalamic neuroinflammation and consequently improved hypothalamic insulin resistance. Moreover, semaglutide promoted the growth of acetate-producing bacteria, high levels of hypothalamic acetate, and increased GPR43+/POMC+ neurons, thus contributing to the restoration of hypothalamic anorexigenic signaling pathways.

Materials and methods

Animals and diets

The local Ethics Committee approved the study and procedures for Animal Use under see number 190/2023 CEUA-FIOCRUZ. Mice male C57BL/6 J (8–10 weeks, $n = 45$) were supplied by Instituto Aggeu Magalhães. They were housed and acclimatized for a week in ventilated cages with controlled temperature (22 ± 1 °C), humidity (60 ± 10%) and light (12:12 h light/dark cycle) with free access to food and water.

After this period, the animals were randomly divided into three experimental groups ($n = 15$/group) and followed for 18 weeks: control (control diet, produced by PragSolucões®, AIN-93G), HFD and HFD + Semaglutide (a diet rich in 60% fat, PragSolucões®, AIN-93 M).

In the 13th week, the HFD + Semaglutide (Ozempic ®—0.05 mg/Kg—translational dose) was administered intraperitoneally every 7 days for 6 weeks and underwent treatment subcutaneously, as described (Robinson et al. 2019). The other groups received a vehicle solution i.p., once a week.

Body weight (BW), waist circumference (WC) and food intake (FI)

Food intake was calculated daily in the 18th week by subtracting the amounts of food offered and food not consumed. Body weight was measured weekly. Waist circumference was measured around the midpoint of the abdomen.

Tissue collection

Mice were euthanized under anesthesia using intraperitoneal Ketamina 240 mg/kg and Xylazine 30 mg/kg. Next, cervical vessels were sectioned rapidly, blood was collected by cardiac puncture (without anticoagulant) and centrifuged at 2300 relative centrifugal force (RCF) for 10 min, and sera were separated and stored at—20 °C ($n = 6$) for biochemical measurements. The intestinal colon and brain of mice were immediately dissected. The hypothalamus was removed and frozen at—80 °C for molecular analysis ($n = 9$). Other brains ($n = 6$) were fixed in a 4% paraformaldehyde (PFA, 0.1 M phosphate buffer, PBS, pH 7.4), embedded in paraffin and cut into 5 μm coronal sections.

Biochemical analysis serum and quantification of acetate in hypothalamus

The glucose level (Labtest Diagnótica S.A®, MG, Brazil—Ref. 133), Triglycerides (Labtest Diagnótica S.A®, MG, Brazil—Ref. 87), cholesterol (Labtest Diagnótica S.A®, MG, Brazil—Ref. 76), Low-density lipoprotein cholesterol (LDL-c) (Labtest Diagnótica S.A®, MG, Brazil—Ref.146) were determined by enzymatic system according to the manufacturer's instructions.

Insulin (Elabscience®, E-EL-M1382), LPS (Fine Test®, Wuhan, China EU3126), and IL-1β (Thermofisher, BMS6002, Vienna, Austria) were determined by enzymatic systems, respectively. Results were expressed as mean ± DP using GraphPad Prism V6.0. Insulin resistance (HOMA-IR) was calculated using the following formula: fasting insulin (μU/mL) × plasma glucose (mmol/L)/22.5 (Obadia et al. 2022).

To measure the acetate concentration in hypothalamus, the samples were homogenized in an extraction solution, and 10-µL hypothalamus content solution were analyzed with an acetate assay kit (Bioassay Systems, USA) using a Multiskan™ FC Microplate Photometer (Thermo Fisher Scientific, USA) spectrofluorometer according to the manufacturer's instructions.

Immunohistochemistry

The sections were treated with 20-mM citrate buffer at pH 6.0 for antigen retrieval and heated to 100 °C for 30 min. Subsequently, the sections were incubated with 3% H2O2 for 30 min to block peroxidase and then 5% BSA for 1 h. Following this, the sections were incubated with primary antibodies, including GFAP (Novus Biological, catalog number NB300-141) at a dilution of 1: 100 and Iba1 (Wako, catalog number 016–20001) at a dilution of 1: 500, overnight at 4 °C and then for 1 h with biotin-conjugated secondary anti-mouse/anti-rabbit IgG antibody. Immunohistochemical reactions were amplified using the Kit Dako LSAB + System-HRP (Dako Universal LSAB® + Kit, Peroxidase), revealed with 3'-3-diaminobenzidine (DAB), and counterstained with Harris Hematoxylin. The slides were counterstained in hematoxylin. Positive staining resulted in a brown reaction product. Negative controls were treated as above, but with the omission of the first antibody. Five pictures/group at the same magnification were quantitatively analyzed (GNU Image Manipulation Program, UNIX platforms).

Immunofluorescence

The samples (three animals/per group) were embedded in paraffin, and the Sects. (5 µm) were cut using a RM 2035 microtome (Reichert S, Leica) and mounted on glass slides, rehydrated, and treated with 20-mM citrate buffer (at pH 6.0) at 100 °C for 30 min. The primary antibodies were anti-POMC antibody (Abcam, catalog number ab32893) at a dilution 1:100, anti-GPR43 antibody (Biologic Science, catalog number bs13563) at a dilution of 1:100, GLP-1R antibody (Novus Biological, catalog number NLS1205) at a dilution of 1:100. The primary antibodies were incubated overnight and then incubated with polyclonal fluor 488- and 546-conjugated secondary antibodies against rabbit and mouse immunoglobulin for 1 h. The slices were washed, mounted in Prolong® medium, observed under a fluorescence microscope Leica DMI8 system, and processed with the Leica Application Suite LAS software (Leica Microsystems, Wetzlar, Germany). The number of hypothalamic GPR43+/POMC+ neurons were quantified from six images per group (two images × three animals), and neurons were considered double-positive to POMC and GPR43 when they presented a yellowish-yellow stain (merge).

Western blotting

The samples were rapidly dissected and homogenized in an extraction solution containing protease inhibitor cocktail (10-mM EDTA, Amresco, Solon, USA; 2-mM phenylmethane sulfonyl fluoride, 100-mM NaF, 10 mM sodium pyrophosphate, 10-mM NaVO4, 10 µg of aprotinin/mL and 100 mM Tris, pH 7.4—Sigma—Aldrich). The samples (four animals/per group) were mixed and homogenized to form a pool for each group. The homogenates were centrifuged and frozen at − 80 °C. The proteins (20 µg/µL) were separated on sodium dodecyl sulfate (SDS) polyacrylamide by gel electrophoresis under reduced conditions and were then transferred electrophoretically onto the nitrocellulose membrane (OmniPage mini-vertical protein electrophoresis, Cleaver Scientific). After blocking with 3% BSA, the membranes were incubated overnight with antibodies against to: IL-1β (dilution of 1:500, Genway, catalog number: GWB-BBP232), p-JNK (dilution of 1:1000, Santa Cruz, catalog number: sc-6254), PI3K p85 alpha (phospho Y607) (dilution of 1:500, Abcam, catalog number: ab182651), AKT (phospho T308) (dilution of 1:500, Abcam, catalog number: ab38449), AMPKα-Phospho (Thr172) (dilution of 1:1000, Cell signaling, catalog number: #2535S), TLR-4 (dilution of 1:1000, Abcam, catalog number: Ab13556), TNF-α (dilution of 1:1000, R&D, catalog number: AF 410-NA), Nitrotyrosine (dilution of 1:1000, R&D, catalog number: Mab3248), Occludin (dilution of 1:1000, Santa Cruz, catalog number: sc-133256), NFkB-p65 (dilution of 1:1000, Cell Signalling, catalog number: cs-3033), MMP-9 (dilution of 1:1000, Santa Cruz, catalog number: sc-133256), MMP-9 (dilution of 1:1000, Abcam, catalog number: Ab110186), GPR-43 (dilution of 1:500, Bioss Antibodies, catalog number: bs-1356r), MyD 88 (dilution of 1:1000, Abcam, catalog number: Ab-2064), p-IkB-α (dilution of 1:1000, Santa Cruz, catalog number: sc-371), p-IRS (dilution of 1:500, Invitrogen, catalog number: PA11054), SIRT (dilution of 1:1000, Santa Cruz, catalog number: sc-74465), POMC (dilution of 1:1000, Abcam, catalog number: ab-32893) and FoxO-1 (dilution of 1:1000, Santa Cruz, catalog number: sc-34890). All primary antibodies were diluted in blocking solution (5% BSA, 0.02% Tris phosphate-buffered, and 0.01% Tween). After washing, the membranes were incubated with peroxidase-conjugated anti-rabbit horseradish (HRP) (dilution of 1:8000, Sigma-Aldrich, catalog number: A9169, USA), or anti-rat HRP (1:5000; Sigma-Aldrich, catalog number: A9037, USA), or anti-mouse HRP (1:5000; Sigma-Aldrich, catalog number: A0161, USA). An enhanced chemiluminescence reagent (Super Signal, Pierce, Ref. 34,080) was used to make the labeled protein bands visible in the iBright CL 1000 system (Thermo Fisher Scientific, catalog number: A44241). For quantification, densitometry values were obtained by measuring each band's pixel density using the Image J 1.38 software (NIH, MD, USA). After the visualization of the protein blots with enhanced chemiluminescence, the protein antibodies were stripped from the membranes, which were reprobed with the monoclonal anti-β-actin antibody (dilution 1:2000, Sigma-Aldrich, catalog number A2228, USA). The results were confirmed by three different repetitions for each investigated protein and statistical analyses were performed with these obtained values.

Gut microbial analysis

After euthanasia, feces content (6 mice/group) were collected, after which they were immediately stored − 80 °C for further and individually detection. The Total DNA extraction was performed by Neoprospecta Microbiome Technologies (Christoff et al. 2017). The DNA were extracted using magnetic beads and the sequencing library preparation for bacterial identification was prepared using the V3/V4 16S rRNA gene 341F (CCTACGGGRSGCAGCAG) (Wang and Qian 2009) and 806R (GGACTACHVGGGTWTCTAAT) (Caporaso et al. 2012) primers and the samples were sequenced in a MiSeq system (Illumina, USA), using the standard Illumina primers provided by the manufacturer kit. Illumina FASTQ files had the primers trimmed and their accumulated error evaluated (Phred < 20). Besides, clusters with abundances lower than 2 were removed. Taxonomic ranks were allocated using a 16S rRNA accurate sequence database set at a 99% identity level (Christoff et al. 2017) using blastn v.2.6.0+ (Altschul et al. 1990). To determine the bacterial taxonomy that explained the differences between

the groups, data-base data with 16S rRNA sequence precision defined at a 99% identity level using blastn v.2.6.0+. α diversity was analyzed by Shannon indexes and Richness; β diversity was investigated using principal coordinate analysis (PCoA). The relative abundance of the phylum and genus level was used to determine the bacterial community structure.

Statistical analysis

For statistical analysis of the data, we used the Graph pad prism v 6.01 program. Parametric data were analyzed using one-way ANOVA, followed by Tukey's post-test. Data were represented by mean ± SD; Probability values lower than 0.05 were considered significant. For statistical analysis of the microbiome, we assessed Alpha diversity using Hill's diversity series (Hill 1973), using different values of q: $q=0$ represents richness, $q=1$ corresponds to Shannon's entropy and $q=2$ means the Reciprocal index by Simpson. To discern variations in taxonomic profiles between experimental groups, we performed beta diversity analyzes via Principal Coordinate Analysis (PCoA), transformed into logarithmic ratio using the Bray–Curtis dissimilarity metric. These analytical procedures were performed in the R environment using the vegan package.

Results

Effect of semaglutide on reducing body weight (BW) gain and waist circumference in HFD-fed male C57BL/6 J mice

To evaluate beneficial metabolic effects of the semaglutide, male C57BL/6 J mice were fed either a control or HFD for 18 weeks. In the 12th week, the HFD-fed mice were further divided into 2 groups HFD and HFD + semaglutide. Figure 1 shows that increased BW in the HFD group reached statistical significance from the 4th to 18th week, compared to the control group. Interestingly, mice fed a high-fat diet (HFD) and treated with semaglutide, showed reduced BW since 14th week compared to the HFD group (Fig. 1A). Notably, although HFD + semaglutide mice lost BW after treatment, they did not achieve the basal BW of the control mice. Moreover, at week 18th semaglutide treatment significantly suppressed food intake compared with the control ($p=0.0002$) and HFD ($p<0.0001$) groups (Fig. 1B), and reduced waist circumference compared to HFD ($p<0.0001$), however, without a significant difference when compared to control rats ($p=0.2125$, Fig. 1C).

Impact of semaglutide on metabolic parameters in HFD-fed male C57BL/6J mice

Figure 2 shows the metabolic parameters results of the mice from all three groups. Compared with the control group, HFD-fed mice after 18 weeks showed significantly increased serum levels of TG, TC, LDL-c, glucose, insulin and HOMA index (Fig. 2A, F). In contrast, semaglutide treatment reduced HFD-induced dyslipidemia, and lowered plasma TG ($p<0.0001$, Fig. 2A), TC ($p<0.0001$, Fig. 2B), and LDL-c ($p<0.0001$, Fig. 2C). In addition, glucose levels ($p<0.0001$, Fig. 2D), insulin concentration ($p<0.05$, Fig. 2E), and HOMA index ($p<0.0001$, Fig. 2F) were dramatically decreased in response to semaglutide treatment compared to HFD. Furthermore, treatment with semaglutide significantly reduced glucose levels compared to the control animals ($p=0.0018$, Fig. 2D), but did not reduce the TG levels to control baseline levels ($p<0.0001$, Fig. 2A).

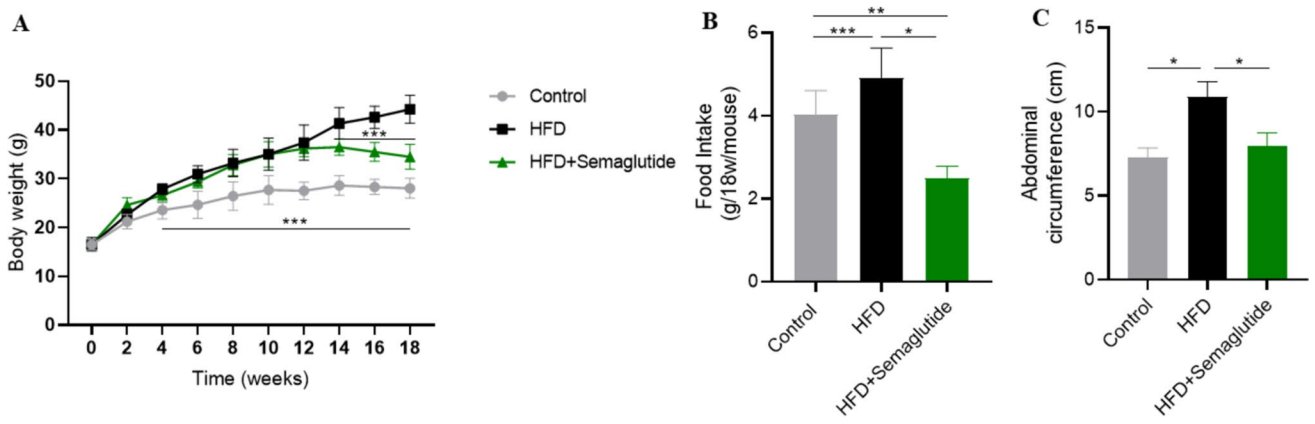

Fig. 1 Semaglutide reduced body weight gain and abdominal circumference in HFD-fed male C57BL/6 J mice. **A** Body weight recording during the first 12 weeks; **B** Food Intake at 18th week; **C** Abdominal circumference at 18th week (cm). Data indicate mean ± SD. $*p<0.0001$, $**p<0.01$, $***p<0.05$ compared to groups; $n=5$ mice/group

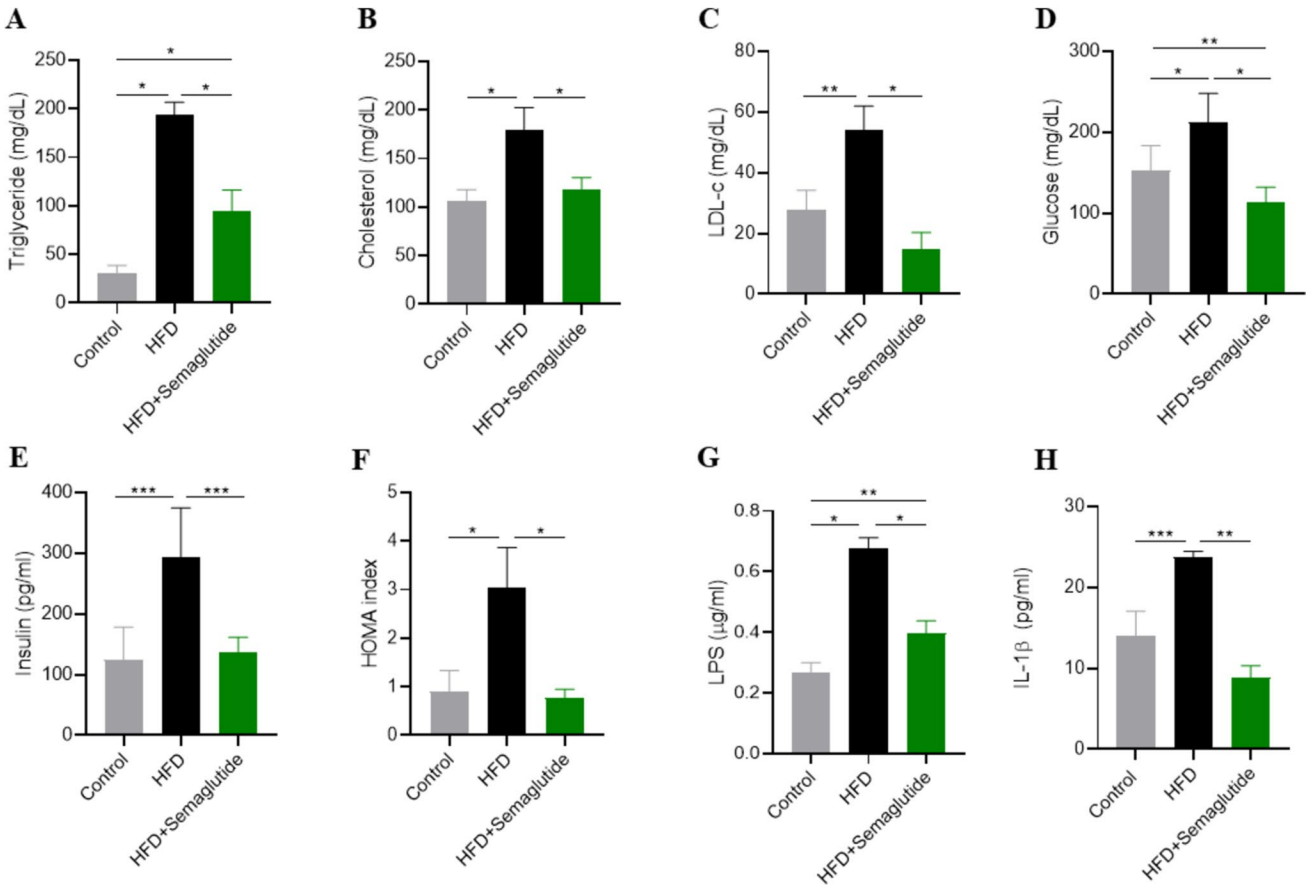

Fig. 2 Semaglutide improve metabolic parameters in HFD-fed male C57BL/6 J mice. **A** Serum total triglycerides (TG, mg/dL); **B** Serum total cholesterol (TC, mg/dL); **C** Serum lipoprotein cholesterol (LDL-c, mg/dL); **D** Serum glucose concentrations (mg/dL); **E** Serum insulin levels (pg/ml); **F** HOMA index; **G** Serum lipopolysaccharide levels (LPS, µg/ml); **H** Serum interleukin-1β levels (IL-1β, pg/ml). Data indicate mean ± SD. $*p < 0.0001$, $**p < 0.01$, $***p < 0.05$ compared to groups; $n = 5$ mice/group

Serum LPS and IL-1β of HFD mice were significantly increased compared to the control group ($p < 0.0001$, $p = 0.0200$ respectively) (Fig. 2G, H), whereas treatment with semaglutide significantly reduced LPS ($p < 0.0001$, Fig. 2G) and IL1β ($p < 0.01$, Fig. 2H) compared to HFD mice. Mice semaglutide-treated present IL-1β similar to the basal levels of the control mice group; however, they exhibited higher LPS levels than the control mice ($p = 0.0021$, Fig. 2G). These results demonstrated that the inflammation HFD-induced can be reduced by semaglutide treatment.

Gut microbiome structural changes determined by 16S rRNA sequencing

The alpha-diversity analyses (Exponential Shannon, reciprocal Simpson index, and Richness) showed a lower bacterial richness and diversity level in the HFD-fed group compared to the control and HFD + Semaglutide groups (Fig. 3A–C). In response to semaglutide treatment, gut microbial diversity and richness were significantly increased compared to HFD and control groups (Fig. 3B, C). In contrast, the PCoA plots (beta-diversity) demonstrated a significant difference between the abundance of groups (Fig. 3D).

In the control the dominant phyla group were Bacteroidetes, Firmicutes and Actinobacteria (Fig. 4A). Regarding phylum analysis, an increase in the average proportion of Bacteroidetes and a decrease in Firmicutes were observed in HFD mice compared to control mice (Fig. 4B, C). In contrast, semaglutide treatment promoted shifts in the HFD mouse gut microbiome, increasing alpha diversity (Fig. 3A–C). Semaglutide increased the proportion of Bacteriodetes and decreased the proportion of Firmicutes (Fig. 4B, C). Furthermore, semaglutide treatment increased taxa Deferribacteria and Proteobacteria compared to the control and HFD-fed groups (Fig. 4A).

At the level of bacterial genera, HFD mice had a significant increase in the relative abundance of *Faecalibaculum* and *Roseburia*, which are members of the phylum Firmicutes, and had a significant reduction in the abundance of members belonging to the phylum Bacteroidetes, driven

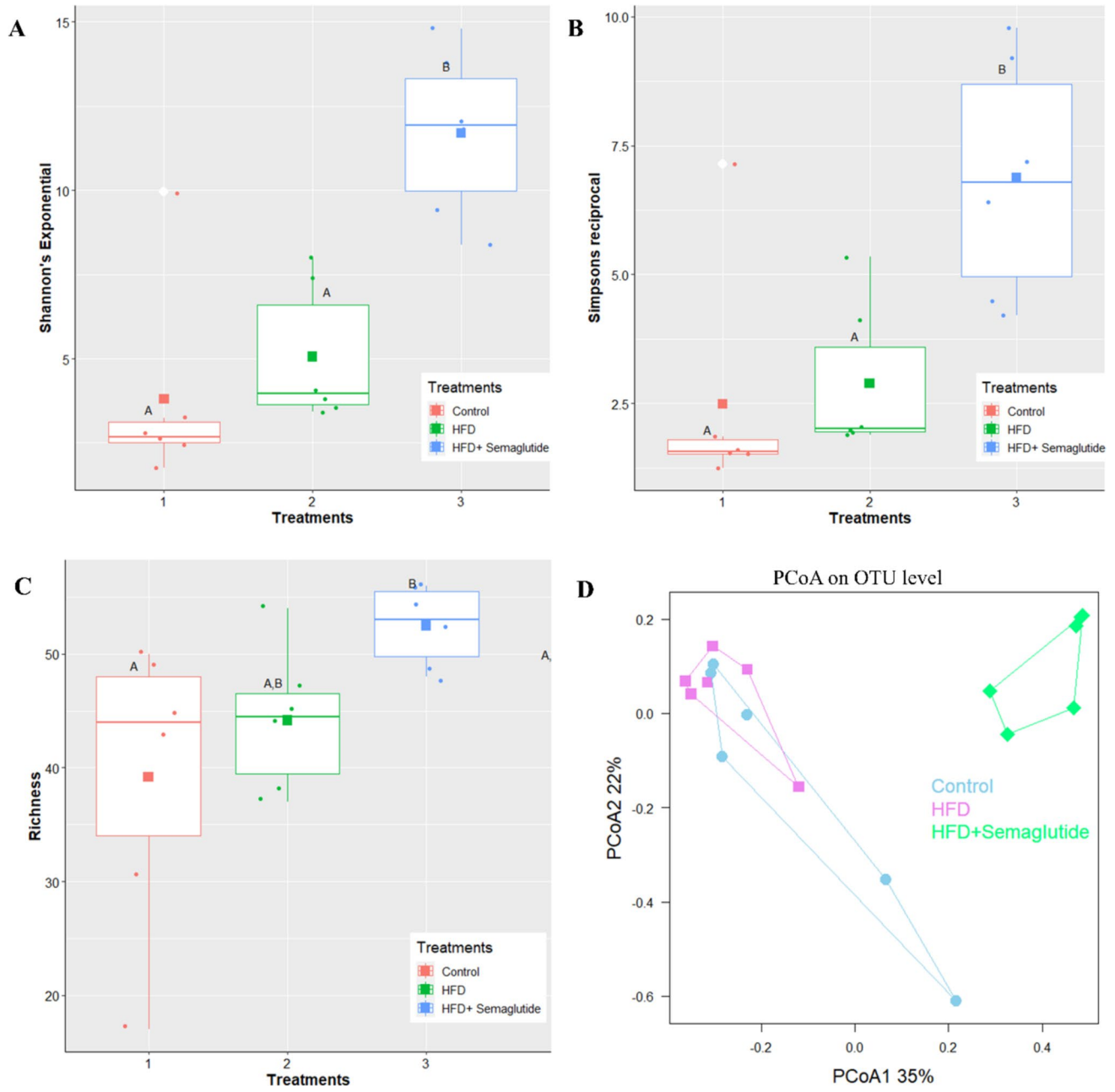

Fig. 3 Semaglutide altered the structure of gut microbiota in HFD-fed mice. **A**–**C**, Shannon, Simpson, and Sobs were determined to assess the α-diversity of gut microbiota. **D** Principal coordinate analysis (PCoA) on OTU level to assess the β-diversity of gut microbiota. Statistical analysis was performed using One-way ANOVA ($n=6$ per group)

by a substantial loss of the genera *Bacteroides* and *Blautia* (Fig. 4D–H). In relation to the species, HFD-fed mice showed high levels of Faecalibaculum rodentium, Lactobacillus johnsonii, and Lachnospiraceae bacterium (Fig. 4I).

Comparisons of samples from HFD + semaglutide to the HFD group revealed an increase of Bacteroides, Blautia, Duncaniella, Mucispirillum (Fig. 4D). The relative abundance of the genera *Bacteroides* and *Blautia* were

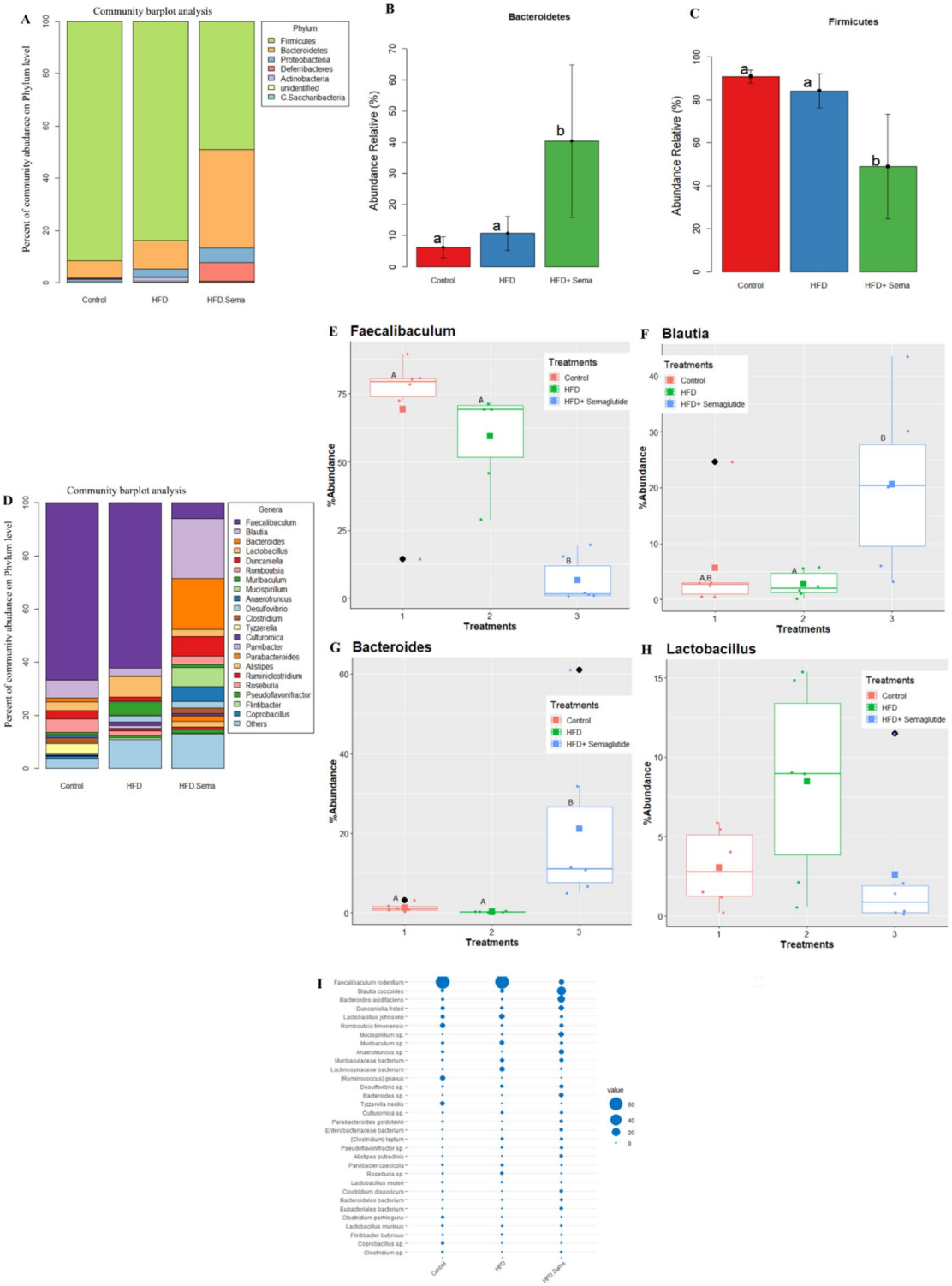

Fig. 4 Semaglutide altered the composition of the gut microbiota HFD-fed mice. **A** Community barplot analysis on phylum level. **B**, **C** Mean relative (bar plot) of 16S rDNA frequencies of Bacteroidetes and Firmicutes phyla. **D** Community barplot analysis on genus level. **E**–**H** Mean relative (bar plot) of 16S rDNA frequencies of Faecalibaculum, Blautia, Bacterioides and Lactobacillus genera. Statistical analysis was performed using One-way ANOVA ($n = 6$ per group)

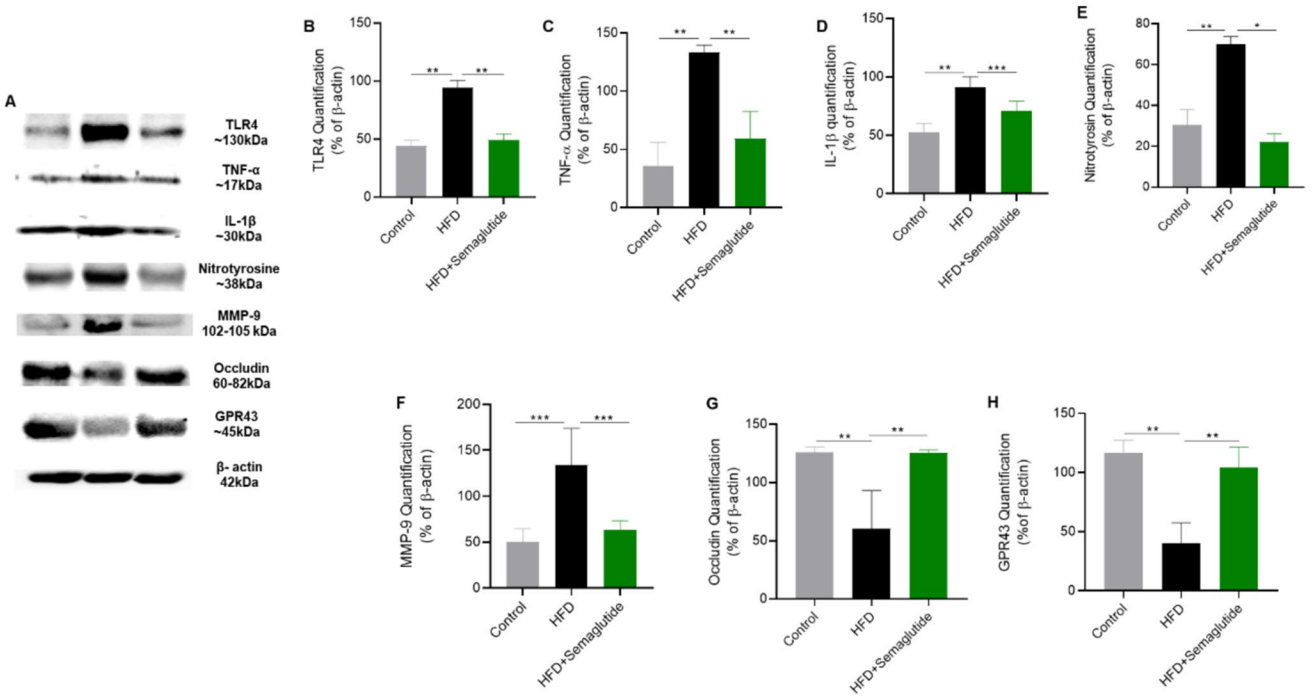

Fig. 5 Semaglutide reduced colonic pro-inflammatory cytokines production and restored the gut barrier integrity. **A** The protein levels of TLR4, TNF-α, IL-1β, Nitrotyrosine, MMP-9, Occludin, GPR43, β-actin were detected by the western blot in the colon ($n=4$/group). **B**–**H** Pixel density quantification of bands. The columns represent the mean ± SD of the protein investigated. One-way ANOVA statistical tests of variance $*p<0.0001$, $**p<0.01$, $***p<0.05$ compared to groups

significantly increased in the semaglutide-treated mice compared to the HFD group (Fig. 4F, G). At the species level, *Blautia coccoides*, *Bacteroides acidifaciens*, *Duncaniella freteri* were significantly increased and *Faecalibaculum rodentium*, *Lachnospiraceae bacterium* were reduced after semaglutide treatment (Fig. 4I).

Semaglutide treatment ameliorated the gut inflammation and restored the colonic integrity in HFD mice

Our analysis of molecular markers of inflammation and colonic integrity in the intestine, as depicted in Fig. 4, revealed a significant increase in TLR4, TNF-α, IL-1β, and nitrotyrosine levels in HFD-fed mice compared to the control group ($p<0.01$, Fig. 5B–E), indicating intestinal inflammation. However, treatment with Semaglutide significantly ameliorated intestinal inflammation, decreasing the expression of TLR4, TNF-α, IL-1β, and nitrotyrosine compared to untreated obese mice ($p<0.05$, Fig. 5B–E). No significative difference was observed between treated-semaglutide and control mice ($p>0.05$).

The intestinal inflammation caused by HFD significantly increased the expression of matrix metalloproteinase-9 (MMP-9), which contributed to the gut inflammation ($p=0.0154$, Fig. 5F). It significantly decreased the expression of occludin ($p=0.0024$, Fig. 5G) compared to the control group. In contrast, semaglutide significantly reduced the expression of MMP-9 ($p=0.0316$, Fig. 5F) and significantly increased the levels of occludin in the distal colon ($p=0.0025$, Fig. 5G) compared to the HFD group. No significant difference was observed between treated-semaglutide and control mice ($p=0.8107$).

The HFD significantly decreased gut GPR43 expression compared to the control ($p=0.0021$, Fig. 5H). In contrast, the treatment with semaglutide significantly prevented the decrease of GPR43 in obese mice ($p=0.0052$, Fig. 5H). No significant difference was observed between treated-semaglutide and control mice concerning the GPR43 expression ($p=0.6098$).

Semaglutide attenuated the hypothalamic glial reactivity in HFD-fed male C57BL/6J mice

In the hypothalamus, the HFD-fed mice significantly increased the glial fibrillary acidic protein (GFAP) positive cells compared to the control group ($p<0.0001$, Fig. 6A, B). As seen in Fig. 5A, the treatment with semaglutide significantly attenuated the reactive gliosis ($p<0.0001$, Fig. 6A, B). No significant difference was observed between

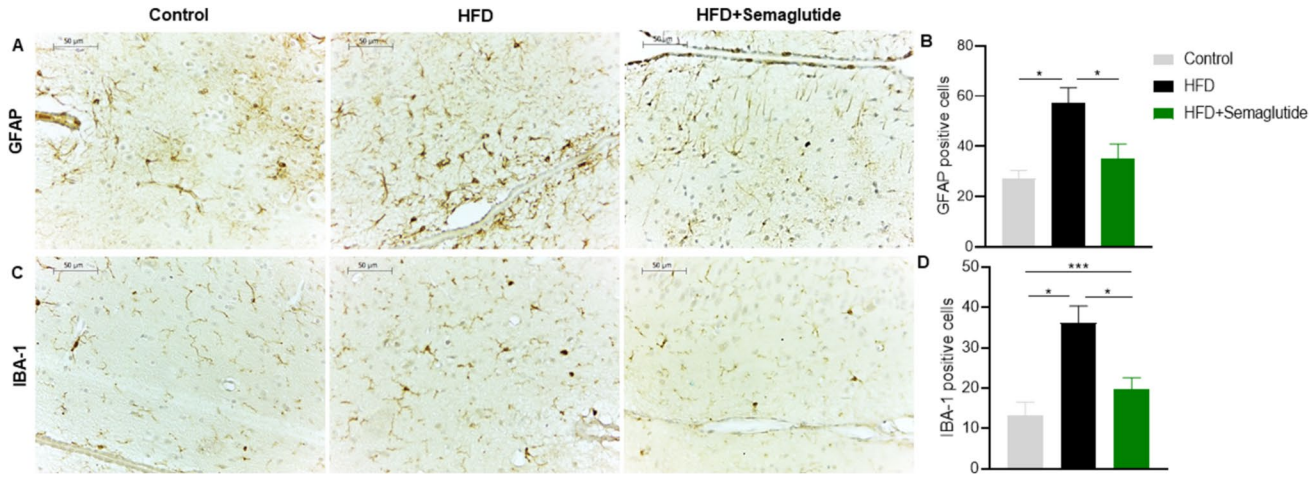

Fig. 6 Immunohistochemical analysis of hypothalamus for GFAP and IBA-1 in HFD-fed male C57BL/6J mice. Positive immunoreactivity is indicated by dark brown color: labeling representative images for **A** GFAP; **B** Graphical representation of GFAP positive cells number; labeling representative images for **C** IBA-1; and **D** Graphical representation of the IBA-1 positive cells number. One-way ANOVA statistical tests of variance $*p < 0.0001, **p < 0.01, ***p < 0.05$ compared to groups ($n = 12$/group), 400× magnification, scale bar = 50 µm (color figure online)

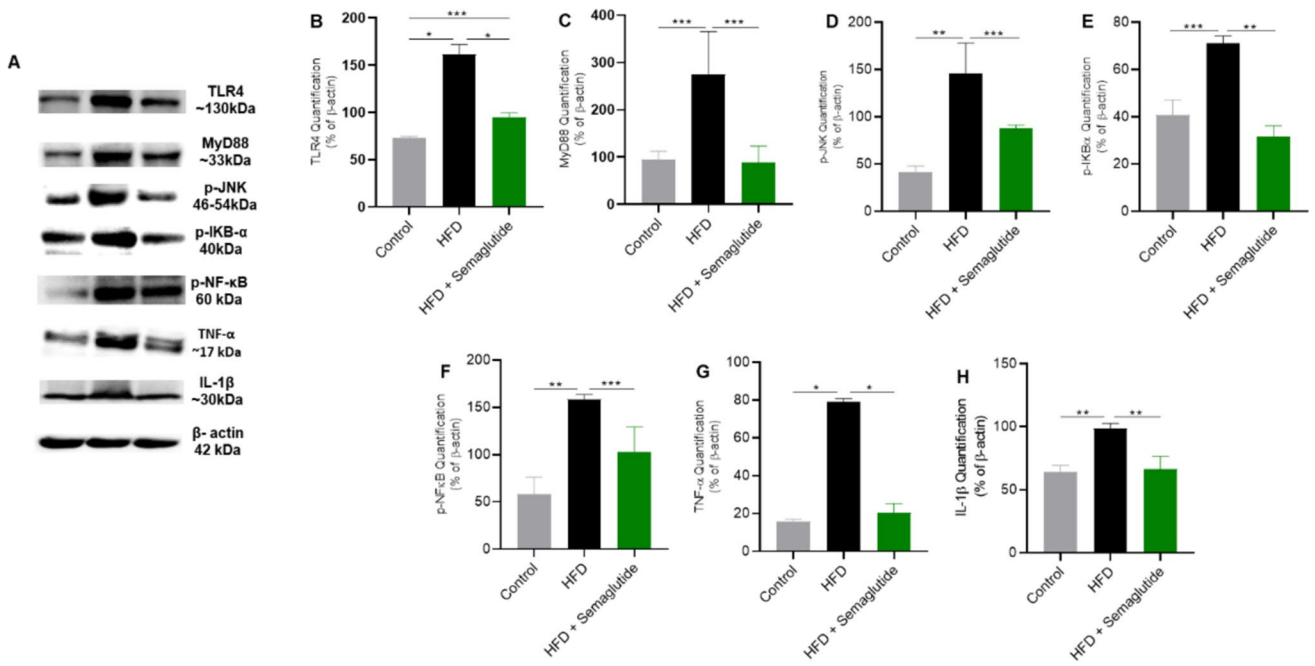

Fig. 7 Semaglutide treatment reduced TLR4/NF-kB inflammatory pathway in the hypothalamus. **A** The protein levels of TLR4, MyD88, p-JNK, p-IkB-α, p-NFkB, TNF-α, IL-1β and β-actin were detected by the western blot in the hypothalamus ($n = 4$/group). **B**–**H** pixel density quantificatiion of bands. The columns represent the mean ± SD of the protein investigated. One-way ANOVA statistical tests of variance $*p < 0.0001, **p < 0.01, ***p < 0.05$ compared to groups

treated-semaglutide group and control mice in relation to the GFAP positive cells ($p = 0.0812$).

Mice fed a HFD also significantly increased the ionized calcium-binding adapter molecule 1 (IBA-1) positive cells in relation to the control group ($p < 0.0001$, Fig. 6C, D). In contrast, treatment with semaglutide significantly reduced IBA-1 positive cells ($p < 0.0001$, Fig. 6C, D). Despite treated-semaglutide mice reduced IBA-1 after treatment, there was no significant difference compared to the control mice ($p = 0.0335$).

Treatment with semaglutide reduces inflammation in the hypothalamus by decreasing TLR4/MyD88/NF-κB signaling

Our data show that the HFD group has significantly increased TLR4, MyD88, p-JNK, p-IKBα, p-NFκB, TNF-α, and IL-1β levels compared to the control group ($p < 0.05$, Fig. 7A–H), indicating the hypothalamic inflammation. On the other hand, semaglutide treatment ameliorated the hypothalamic inflammation, decreasing the TLR4, MyD88, p-JNK, p-IKBα, p-NF-κB, TNF-α, and IL-1β significantly when compared to the HFD group ($p < 0.05$, Fig. 7A–H). Except for TLR4 ($p = 0.0140$), no significant differences were observed between the semaglutide-treated group and control mice relative to MyD88, p-JNK, p-IKBα, p-NFκB, TNF-α mice and IL-1β ($p > 0.05$).

Semaglutide modulated the GPR43/IRS/PI3K/AKT/AMPK/SIRT/FoxO-1/POMC signaling pathway in the hypothalamus of obese animals

The HFD group showed a reduced expression of the receptor for SCFAs, GPR43, in the hypothalamus, compared to the control group ($p < 0.0001$, Fig. 8A, B). In contrast, in the HFD group treated with semaglutide there was an increase in GPR43 levels compared to the HFD group ($p = 0.0090$, Fig. 8A, B).

As observed, protein expression IRS was reduced in the HFD group, compared to the control group ($p < 0.0001$, Fig. 8A, C). In contrast, the HFD + semaglutide group showed an increase in IRS expression in the hypothalamus compared to the HFD group ($p < 0.0001$, Fig. 8A, C).

There were also significantly reduced p-PI3K levels in the HFD group compared to the control group ($p < 0.0001$, Fig. 8A, D). However, the HFD group treated with semaglutide showed a substantial increase in p-PI3K levels compared to the HFD group ($p < 0.0001$, Fig. 8A, D).

The p-AKT levels decreased in the HFD group compared to the control group ($p < 0.0001$, Fig. 8A, E). Similarly, the HFD group treated with semaglutide showed no significantly increased p-AKT levels compared to the HFD group ($p < 0.0173$, Fig. 8A, E).

Furthermore, there was also a reduction in p-AMPK-α levels in the HFD group compared to the control group

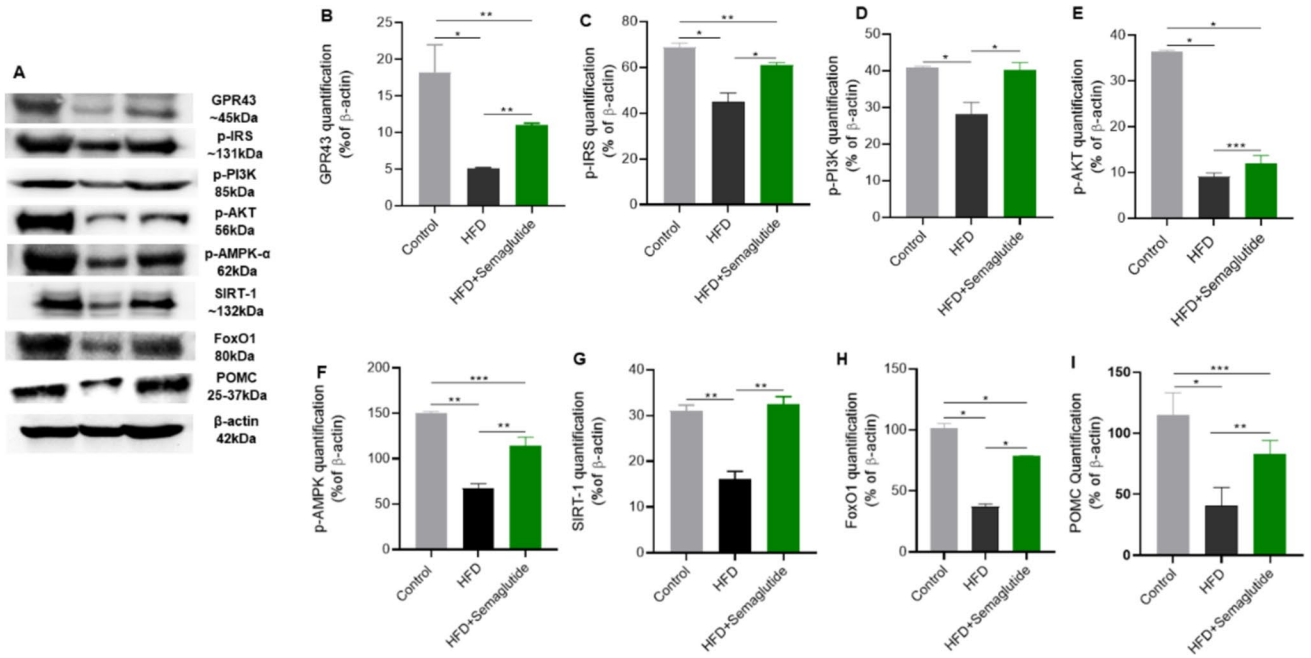

Fig. 8 Semaglutide improvement of anorexigenic signaling in obese mice. **A** The protein levels of GPR43, p-IRS, p-PI3K, p-AKT, p-AMPK-α, SIRT-1, FoxO-1, POMC and β-actin were detected by the western blot in the hypothalamus ($n = 4$/group). **B**–**I** pixel density quantification of bands. The columns represent the mean ± SD of the protein investigated. One-way ANOVA statistical tests of variance $*p < 0.0001$, $**p < 0.01$, $***p < 0.05$ compared to groups

($p = 0.0019$, Fig. 8A, F). In contrast, the semaglutide treatment increased p-AMPK levels compared to the HFD group ($p = 0.0099$, Fig. 8A, F).

The HFD group showed a reduction in SIRT-1 levels compared to the control group ($p = 0.0043$, Fig. 8A, G), and treatment with semaglutide counteracted improving SIRT-1 expression ($p = 0.0032$, Fig. 8A, G).

Moreover, the HFD group showed reduced levels of FoxO-1 compared to the control group ($p < 0.0001$, Fig. 8A, H), whereas the treatment with semaglutide increased FoxO-1 levels compared to the HFD group ($p < 0.0001$, Fig. 8A, H).

POMC expression was reduced in HFD group compared to the control group ($p < 0.0001$, Fig. 8A, I). In contrast, the HFD + semaglutide group showed higher levels of POMC protein expression than the HFD group ($p = 0.0029$, Fig. 8A, I).

No significant differences in the expression of p-PI3K and SIRT were observed between semaglutide-treated and control mice. In contrast, semaglutide treatment did not restore baseline levels of other signaling molecules compared to the control group (Fig. 8).

Semaglutide treatment increased GLP-1R expression in the hypothalamus

The HFD group showed reduced GLP-1R expression compared to the control group ($p < 0.0001$, Fig. 9A, B). When compared with HFD + Semaglutide group, it showed a significant increase to the HFD group ($p = 0.0002$, Fig. 9A, B). No significant difference was observed between treated-semaglutide and control mice in relation to the GLP-1R expression ($p = 0.1244$).

Semaglutide treatment increased co-localization of GPR43 with POMC-positive neurons in the hypothalamus

We also aimed to analyze the effect of semaglutide on the modulation of the expression of GPR43 in POMC neurons. The HFD-fed mice presented reduced numbers of $POMC^+$ neurons compared to the control group ($p < 0.0001$, Fig. 10A, D), and treatment with semaglutide significantly restored the number of $POMC^+$ neurons ($p = 0.0001$, Fig. 10A, D). Similarly, HFD-fed mice presented a reduced number of GPR43 + neurons compared to the control and HFD + semaglutide groups ($p < 0.01$, Fig. 10B, E). In contrast, the treatment with semaglutide increased the number of $GPR43^+$ neurons ($p = 0.0001$, Fig. 10B, E) compared to the HFD-fed group. The co-localization demonstrated that HFD mice presented reduced $POMC^+$ $GPR43^+$ neurons compared to the control group ($p < 0.0001$, Fig. 10C, F). On the other hand, semaglutide-treated mice showed a significantly higher number of POMC+ GPR43+ neurons than the HFD group ($p < 0.0001$, Fig. 10C, F). No significant difference was between treated-semaglutide and control mice in relation to the $POMC^+$ $GPR43^+$ neurons ($p = 0.0055$).

Semaglutide increases hypothalamic acetate levels in high-fat diet-induced obese mice

The results of the effect of semaglutide on the gut microbiota diversity revealed the growth of acetate-producers' bacteria

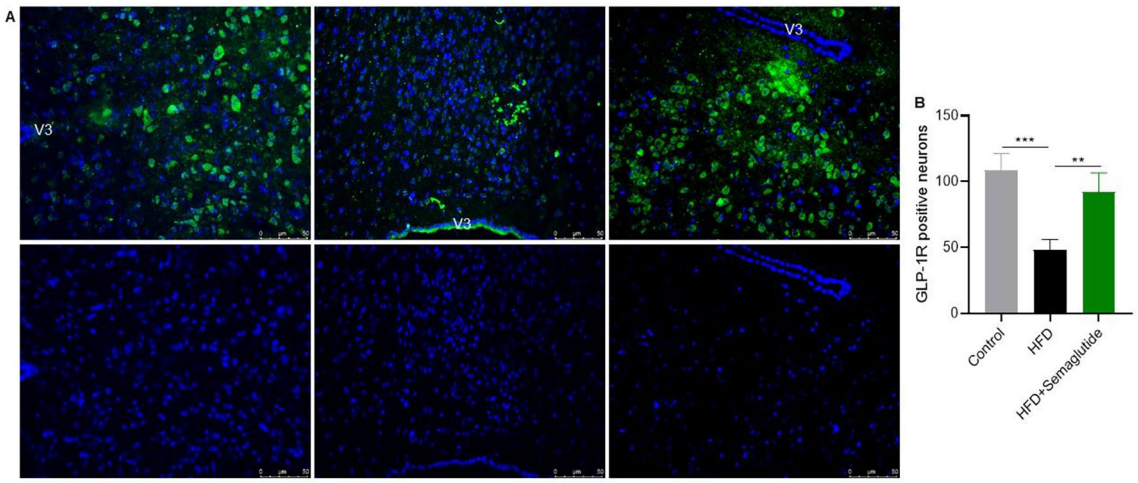

Fig. 9 Semaglutide increases GLP-1R expression in the ARC region of the hypothalamus in obese mice. **A** Representative images of immunofluorescence staining of neuronal GLP-1R (green); **B** the number of GLP-1R-positive cells ($n = 9$/group). V3: third ventricle. Scale bars: 50 µm. Data denote significant differences, $*p < 0.0001$, $**p < 0.01$, $***p < 0.05$ compared to groups. (ANOVA followed by Tukey's Multiple) (color figure online)

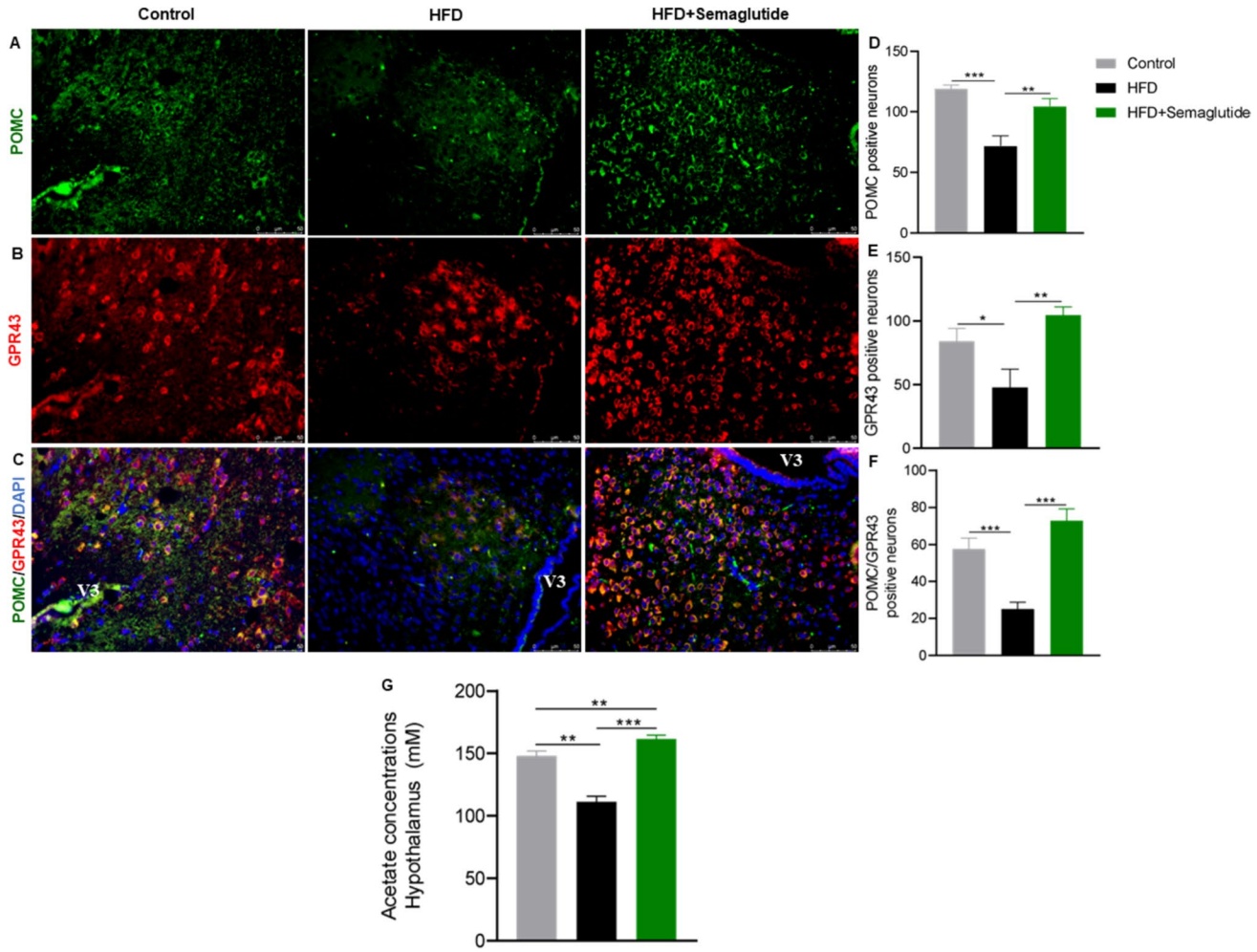

Fig. 10 Semaglutide induced GPR43 expression in POMC neurons and increased hypothalamic acetate concentrations in HFD-fed C57BL/6J mice. **A** representative images of POMC neurons (green); **B** total POMC-positive neurons, **C** representative images of GPR43 (red); **D** total GPR43-expressing neurons; (E) Colocalization of GPR43 with POMC neurons in the arcuate nucleus (yellow), **F** total active POMC/GRPR43 neurons ($n=9$/group). **G** Comparison of acetate concentrations in the hypothalamus ($n=4$/group). V3: third ventricle. Scale bars: 50 µm. Data denote significant differences, $*p<0.0001$, $**p<0.01$, $***p<0.05$ compared to groups (ANOVA, followed by Tukey's Multiple) (color figure online)

(*Bacteroides acidifaciens*, and *Blautia coccoides*). In addition to exerting local effects on the colon and peripheral tissues, acetate can cross the BBB to the central nervous system and have neuroactive properties through GPR43 receptors (Silva et al. 2020b). The HFD group showed significantly lower hypothalamic acetate levels than the control group ($p=0.0003$, Fig. 10G). On the other hand, the semaglutide administration significantly increased the acetate level in the hypothalamic tissue compared to the HFD group ($p<0.0001$, Fig. 10G). Interestingly, semaglutide induced higher levels of acetate than the control group ($p=0.0157$, Fig. 10G).

Discussion

Evidence suggests that bidirectional communication along the gut–brain axis is crucial to the synergy between microbiota and gut–brain signaling pathways through neural, endocrine, immune, and humoral links (Cryan et al. 2019). On the other hand, the HFD promotes an imbalance in the composition of the intestinal bacterial microbiota (dysbiosis) and influences the expression of inflammatory factors (De La Serre et al. 2010). Obese individuals, as well as experimental models of obesity (HFD), present changes in the

composition of the intestinal microbiota with an increase in the Firmicutes/Bacteroidetes ratio, therefore favoring the growth of pathogenic bacteria and facilitating the passage of bacterial toxins, such as lipopolysaccharide (LPS), into the circulation. LPS, through the activation of Toll-like receptors 4 (TLR4), triggers the activation of the transcription factor NF-κB that induces an increase in the expression of intestinal pro-inflammatory cytokines, such as IL-1β and TNFα, which can reach the systemic circulation and enter the CNS, contributing to neuroinflammation (Agustí et al. 2018; Fiebich et al. 2018). Furthermore, matrix metalloproteinase-9 (MMP-9) is an important factor contributing to intestinal inflammation, increasing intestinal permeability by reducing tight junctions (Al-Sadi et al. 2021). These junctions are composed of intercellular adhesive proteins, such as occludin, which provide a vital barrier function. Furthermore, pro-inflammatory cytokines, such as IL-1β, reduce the expression of these proteins, contributing to the leaky gut (Al-Sadi et al. 2011; Agustí et al. 2018).

The present results show that mice fed HFD exhibited high intestinal levels of TLR4, NF-kB, TNF-α, IL-1β, MMP-9, and nitrotyrosine and low levels of occludin, indicating gut inflammation and permeability, resulting in higher IL-1β and LPS serum levels. HFD-fed mice also showed significantly increased TG, TC, LDL-c serum levels, glucose, insulin and HOMA index. In contrast, treatment with the GLP-1R agonist, semaglutide, reduced dyslipidemia, insulin resistance, IL-1β, LPS serum levels, and intestinal inflammatory markers. Moreover, semaglutide reduced BW and waist circumference in HFD-fed mice. Recent results had suggested that semaglutide can modulate energetic homeostasis by directly acting on hypothalamic and hindbrain GLP-1R and neural pathways involved in food intake (Gabery et al. 2020b).

The ARC is the "first-order center" for food intake regulation within the hypothalamus. It contains two groups of neurons, anorexigenic proopiomelanocortin (POMC)/cocaine-regulated transcription and amphetamine (CART) neurons and orexigenic agouti-related peptide (AgRP)/neuropeptide Y (NPY) neurons, which are functionally antagonistic (Morton et al. 2006). The transcription factor Factor Forkhead Box 01 (FoxO-1) is an integral component of the insulin and insulin-like growth factor signaling pathway and is expressed in both types of neurons. FoxO-1 is located within the nucleus during starvation and translocated to the cytoplasm after feeding. FoxO-1 promotes the appetite by direct promoter binding to Agrp and Pomc genes, with an activation effect on AgRP, and an inhibitory effect on POMC expression (Du and Zheng 2021b). When secreted insulin or insulin-like growth factors (IGFs) bind to their cell surface receptors, a series of autophosphorylations occur, recruiting INSR substrate 1–4 (IRS1–4) and phosphatidylinositol 3-kinase (PI3K). PI3K increases local concentrations of phosphatidylinositol (3,4,5)-trisphosphate (PIP3). PIP3 is a second messenger that activates phosphoinositide-dependent kinase 1 (PDK1) and protein kinase B (Akt or PKB). Active Akt translocates to the nucleus, where it phosphorylates FoxO-1, leading to the 14-3-3 dimer binding and inducing the translocation of FoxO-1 to the cytoplasm.

The effect of a high fat/calorie diet is well-recognized in generating reactive oxygen species (ROS) and pro-inflammatory cytokines (IL-1β, IL-6, TNF-α) that are potent deregulators of hypothalamic control of energy homeostasis. Experimental models' mouse of obesity showed that overconsumption of a fat-rich diet results in increased pro-inflammatory genes (IL-6 and TNF-α) in the hypothalamus after 4 weeks of HFD; notably, these occurrences of inflammation precede events in peripheral tissues, such as the liver (Thaler et al. 2012). In this context, the fatty acids, especially long-chain saturated fatty acids (SFAs), can cross the BBB (Karmi et al. 2010; Valdearcos et al. 2014). SFAs activate the TLR4/JNK pathway, which triggers the inhibitory phosphorylation of insulin receptor substrate (IRS) proteins at serine 307, promoting the onset of insulin and leptin resistance in the hypothalamus (Martin et al. 2006; Naznin et al. 2015; Jais and Brüning 2017). Consistent with these observations, our data shows that the HFD group had a significant increase of TLR4, MyD88, p-MAPK-p38, p-IKBα, p-NFκB, TNF-α, and IL-1β levels compared to the control group, indicating hypothalamic inflammation. In contrast, the semaglutide intervention abrogated hypothalamic inflammation by reducing the TLR4/MyD88/NFκB signaling pathway.

Inflammatory mediators and increased levels of reactive oxygen species (ROS) activate the c-Jun N-terminal kinase (JNK), which, in turn, phosphorylates the cytoplasmic FoxO-1, inducing the release of FoxO-1 from 14-3-3, dimer and promotes the nuclear translocation of FoxO-1 upregulating its transcriptional activity, despite the phosphorylation by Akt. This misregulation of the FoxO-1 signaling pathways leads to the inhibition of the anorexigenic effects of insulin (Kim et al. 2006), increases adiposity, and promotes weight gain (Susanti et al. 2014).

Moreover, JNK inhibits PI3K, resulting in the FoxO-1 activation and promoting the AgRP/NPY expression, which induces hyperphagia and weight gain (Tsaousidou et al. 2014). The present results showed that semaglutide treatment reduced p-JNK and restored FoxO-1 hypothalamic expression, thus regulating insulin/leptin signaling. In addition, TNF-α and IL-6 levels can also stimulate the expression of proteins of the suppressor of cytokine signaling-3 (SOCS3), a standard inhibitor of insulin and leptin signaling through IKKβ/NF-κB pathway (Romanatto et al. 2007; Zhang et al. 2008; Li et al. 2021).

Sirtuin 1 (SIRT1) is a nutrient-sensing deacetylase activated by high levels of NAD+, which increases during

energetic crises, such as fasting and calorie restriction, and decreases under conditions of high-energy load (Xu et al. 2018). SIRT1 is mainly localized in the nucleus, where it directly deacetylates FoxO-1 and transactivates a series of target genes (Kodani and Nakae 2020). Conversely, SIRT1 is reduced under high-energy conditions, such as high-fat diets. (Nogueiras et al. 2012; Xu et al. 2018). As expected, the HFD mice presented lower levels of hypothalamic SIRT1, whereas treatment with semaglutide restored the SIRT1 expression, thus modulating the energetic systemic homeostasis. On the other hand, inflammatory mediators such as pro-inflammatory cytokines and oxidative stress activate JNK, which directly concentrates SIRT1 in the nucleus, activating orexigenic genes (Nasrin et al. 2009). Our results also showed significantly high levels of pro-inflammatory mediators in the hypothalamus as well as high levels of JNK, which probably overridden the low levels of SIRT-1 observed in HFD mice.

Incretin hormone-based therapies are widely used to improve hyperglycemia in patients with T2DM (Fonseca et al. 2010). GLP-1 is the main hormonal incretin, an anorectic peptide secreted by L cells in response to nutrient intake. Other beneficial effects of GLP-1 are improving the intestinal barrier, stimulating crypt cell fission, and inhibiting pro-inflammatory cytokines released by immune system cells (May et al. 2019). The molecular bases of the inhibitory action of GLP-1 on food intake and BW loss are complex, and the effect of GLP-1 agonists on the hypothalamus is crucial for the anorectic effect. GLP-1 regulates energy homeostasis and feeding behavior by modulating neuronal electrophysiological properties in the CNS, mainly the ARC (Chen et al. 2021; Singh et al. 2022b).

The binding of GLP-1 to its receptor GLP-1R leads to the activation of adenylate cyclase (AC) and subsequently to an increase in cAMP (Müller et al. 2019). In eukaryotic cells, the protein kinase A (PKA) and cAMP-dependent exchange protein (EPAC) are the main downstream cAMP effectors that regulate several physiologic functions, including AMPK activity (Aslam and Ladilov 2022). The AMPK activity is modulated by the energetic conditions and peripheral hormones that control food intake in ARC and paraventricular nucleus PVN. In fasting conditions, AMPK has an orexigenic effect phosphorylating FoxO-1, which activates the transcription of Neuropeptide Y (NPY)/AgRP genes. In turn, the anorectic hormones such as insulin and leptin decrease AMPK phosphorylation via STAT3/PI3K, resulting in the inhibition of Neuropeptide Y (NPY)/AgRP neurons and in the activation of Proopiomelanocortin (POMC) neurons in the ARC, which project to the PVN (Kahn et al. 2005; Martin et al. 2006). The results here showed that HFD-fed mice presented decreased hypothalamic GLP-1R, p-AMPK and POMC levels, which were reverted by semaglutide treatment, suppressing the food intake and weight gain. These results are in agreement to other authors that demonstrated that semaglutide increased POMC expression in the ARC and restored the leptin, amylin, and GLP1 levels (Martins et al. 2023).

SCFAs, such as acetate, propionate, and butyrate, are primary byproducts synthesized by the gut microbiota through anaerobic fermentation of insoluble dietary fibers (Silva et al. 2020b). SCFAs, besides functioning as energy sources, also activate two orphan G-protein coupled receptors (GPCR), GPR41 and GPR43. GPR43 promotes intestinal motility and gut hormone secretion, such as PYY and GLP-1, thereby increasing energy expenditure and improving glucose tolerance (Kimura et al. 2014). GPR43 is expressed in several tissues, including intestine, adipose, and immune tissue, playing an important role in regulating intestinal immunity (Hong et al. 2005; Maslowski et al. 2009; Sina et al. 2009). GPR43 is abundantly expressed in numerous gastrointestinal tract cells where they modulate the intestinal permeability by increasing tight junctions' proteins, such as zonnula occludens and occludin. Accordingly, our results showed that HFD-fed mice presented reduced gut GPR43 and occluding expression, which were reverted in semaglutide tread mice.

In white adipocytes, binding of SCFAs to GPR43 leads to increased leptin expression, whose receptors expressed in neurons of hypothalamic nuclei have a fundamental role in brain–adipose crosstalk to energy homeostasis (Xiao et al. 2019). GPR43 activation also suppresses adipose insulin signaling, inhibiting fat accumulation and stimulating the expenditure of energy by muscles (Kimura et al. 2013). Therefore, GPR43 acts as an energy sensor, controlling excess energy while maintaining metabolic homeostasis. Among the SCFAs, acetate is the most efficient for activating GPR43, followed by propionate and butyrate. Acetate possibly regulates appetite by secretion of gut appetite-suppressing hormones and central hypothalamic mechanisms (Hernández et al. 2019). Frost et al. described HFD-fed mice supplemented for 8 weeks with oligofructose-enriched inulin presented elevated serum acetate derived from the colon, which induced an anorectic signal in the hypothalamic ARC through reduced levels of AMPK (Frost et al. 2014).

The ratio of Firmicutes to Bacteroidetes is increased in diabetic patients and during consumption of high-calorie diets, leading to impaired glucose metabolism and increased obesity; on the other hand, inverting this proportion leads to weight loss and reduced inflammation (Kant et al. 2022). Interestingly, GLP-1R agonists impact the intestinal environment by modulating the intestinal microbiota composition, improving the intestinal barrier, and reducing the production of pro-inflammatory cytokines (Yusta et al. 2015; Abdalqadir and Adeli 2022). Treatments with GLP-1R agonists such as liraglutide, dulaglutide, and semaglutide induce an increase in the proportion of Bacteroidetes to Firmicutes,

as well as gut microbes related to the lean phenotype (Blautia and Akkermansia) (Wang et al. 2016, 2018; Hupa-Breier et al. 2021; Duan et al. 2024).

The present study showed that treatment with semaglutide remodeled the obesity-induced gut dysbiosis, increasing the Bacteriodetes/Firmicutes ratio and the relative abundance of *Bacteroides acidifaciens* and *Blautia coccoides*, which are acetate producers. Notably, there was a significant reduction in the hypothalamic acetate concentration in obese animals compared to the control group. We also demonstrated that semaglutide treatment induced high levels of hypothalamic acetate, which possibly upregulated the expression of hypothalamic GPR43. In the hypothalamic ARC, acetate activates the GPR43 and the downstream PI3K-AKT signaling (Yang et al. 2018) and AKT can also directly phosphorylate AMPK at inhibitory Ser485, thus negatively regulating its activity (Aslam and Ladilov 2022). In addition, Akt, which is common to the insulin/IRS/PI3K pathway, will activate POMC neurons by repressing the FoxO-1, which negatively regulates the transcription of genes such as POMC (Derghal et al. 2019). Our results also showed that semaglutide through IRS/PI3K/AKT signaling also improved the insulin hypothalamic pathway via reduced peripheral insulin resistance, as indicated by HOMA-IR. In addition, the treatment with semaglutide induced a higher number of $POMC^{+}$ / $GPR43^{+}$ neurons in the ARC, confirming the GPR43 pathway in POMC neurons. These results are in agreement with those previously obtained by others (Liu et al. 2017), in which the treatment intravenously with acetate induced anorexia via the upregulation of hypothalamic POMC and GPR43 gene expression.

The relationship between semaglutide and intestinal microbes is environmentally complex, and further studies are still needed to investigate the effects of microbiota or individual bacteria on semaglutide. Semaglutide may influence the composition of the microbiota through its influence on the gastrointestinal tract. For example, many preclinical and clinical studies suggested that GLP-1R agonists can modulate the gut microbial composition by influencing the gastric emptying rate, the gut transit time, and the internal environment of the gut lumen (pH levels and nutrient availability) (Grasset et al. 2017; Montandon and Jornayvaz 2017; Wang et al. 2017; Zhao et al. 2018; Madsen et al. 2019; Shang et al. 2021). Another factor to be considered is the suppression of gut inflammation since GLP-1R is present in immune cells (Abdalqadir and Adeli 2022; Alharbi 2024). GLP-1R activation in gut intraepithelial lymphocytes (IELs) modulates enteric immune responses and is required to modulate a subset of the gut microbiota (Wong et al. 2022). However, the mechanisms of GLP-1R signaling in IELs are just beginning to be understood (Rosario and D'Alessio 2015; Yusta et al. 2015; Chen et al. 2022; Holst et al. 2022; Morrow et al. 2024; Sun et al. 2024). Finally, semaglutide may indirectly influence microbiota by improving glycemic homeostasis, reducing insulin resistance, decreasing intestinal irritation, and promoting a more favorable environment for beneficial microbiota (Mao et al. 2024; Duan et al. 2024). Microbial genomic and metabolomic analyses in healthy animals treated with semaglutide will help to understand whether this drug exerts its direct effects on the microbiota (such as stimulating some microbiota strains and inhibiting others) or whether these effects are due to the improvement of obesity in the host.

Conclusion

Our results showed that a high-fat diet resulted in systemic and CNS inflammation associated with gut dysbiosis, intestinal inflammation, and gut permeability. Furthermore, the HFD significantly impacted weight gain, lipid metabolism, and glucose homeostasis. Semaglutide intervention counteracted dyslipidemia, insulin resistance, serum inflammatory markers, intestinal permeability, and gut inflammation. Semaglutide also reverted the hypothalamic neuroinflammation HDF-induced decreasing TLR4/MyD88/NF-κB signaling, and consequently improving insulin resistance. Moreover, semaglutide modulated the intestinal microbiota, promoting the growth of acetate-producing bacteria, inducing high levels of hypothalamic acetate, and increasing the number of GPR43+/POMC+ neurons. In the ARC, acetate activates the GPR43 and its downstream PI3K-AKT pathway, which activates POMC neurons by repressing the FoxO-1, thus restoring hypothalamic anorexigenic signaling pathways (Fig. 11). Therefore, among the effectors of the multifactorial modulation of hypothalamic energy homeostasis, possibly higher levels of acetate derived from the intestinal microbiota contribute to reducing food intake.

As a limitation of this study, we highlight that fecal transplantation of animals treated with semaglutide could contribute to the confirmation and elucidation of the mechanisms underlying the hypothalamic modulation of food intake. Therefore, additional studies must be conducted to unravel the full range of functions of microbiota

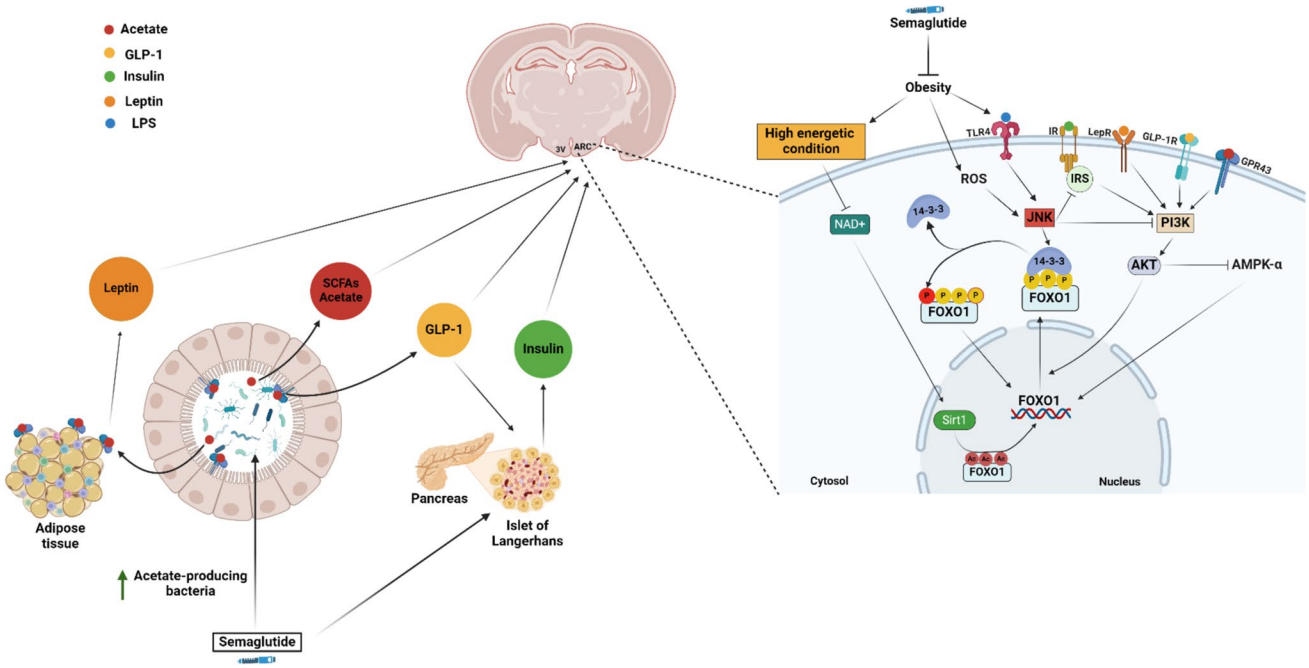

Fig. 11 Food intake modulation by semaglutide—Insulin, growth factors, leptin, and GLP-1 activate the PI3K/Akt signaling pathways that repress FoxO-1 and AMPK, resulting in an anorectic effect through NPY/AgRP decreased expression. On the other hand, obesity deregulates the profile of the intestinal microbiota, promoting intestinal permeability (leaky gut) and allowing LPS and other pro-inflammatory molecules to enter the bloodstream. In the hypothalamic ARC, inflammatory mediators (LPS, TNF-a, IL1-beta, SFAs) and oxidative stress species (ROS) activate JNK that blunt the IRS/PI3K pathway. Furthermore, JNK induces the release of FoxO-1 from the 14-3-3 dimer and promotes its nuclear translocation despite phosphorylation by Akt, promoting increased food intake and body weight gain. Treatment with semaglutide increases the abundance of acetate-producing bacteria in the gut; in turn, the acetate reaches the hypothalamic ARC through circulation and binds to its receptor on first-order neurons, which induces an anorexigenic signal through PI3K/Akt signaling

modulation driven by GLP-1R agonists in the context of metabolic diseases.

Authors' contributions R.S.S. and C.P. conceived the study and design the experiment. R.S.S. performed the main experimental work, analyzed the data, created the figures and drafted the manuscript. All other authors performed experiments, and J. R. B. S performed statistical analysis. C.P. extensively and critically reviewed the manuscript. All authors accepted the final version of the paper.

Funding This work was supported by the Research Excellence Program—Instituto Aggeu Magalhães (IAM-PROEP#400208/2019-9), the Knowledge Generation Program of the Fundação Oswaldo Cruz (FIOCRUZ;#VPPCB-007-FIO-18-2-17), the Institute of Science and Technology of Neuroimmunomodulation (INCT- NIM; # 465489/2014-1) and the National Council for Scientific and Technological Development (CNPq;#301777/2012-8). Institute Pesquisas Aggeu Magalhães, Fundação Oswaldo Cruz (IAM-PROEP# 005-FIO-22).

Data availability The data that support the findings of this study are available from the corresponding author (Peixoto C.A.) upon request.

Declarations

Conflict of interest The authors declare that they have no competing interests.

Ethics approval and consent to participate All experiments were conducted by the Ethical Principles in Animal Experimentation and were accepted by the Ethics Committee on the Use of Animals of the Aggeu Magalhães Institute (CEUA 135/2018—IAM).

Consent for publication This research did not receive any specific grant from funding agencies in the public, commercial, or not-for-profit sectors.

References

Abdalqadir N, Adeli K (2022) GLP-1 and GLP-2 orchestrate intestine integrity, gut microbiota, and immune system Crosstalk. Microorganisms 10

Agustí A, García-Pardo MP, López-Almela I et al (2018) Interplay between the gut-brain axis, obesity and cognitive function. Front Neurosci 12

Alharbi SH (2024) Anti-inflammatory role of glucagon-like peptide 1 receptor agonists and its clinical implications. Ther Adv Endocrinol Metab 15:1–18. https://doi.org/10.1177/20420188231222367

Al-Sadi R, Engers J, Haque M et al (2021) Matrix Metalloproteinase-9 (MMP-9) induced disruption of intestinal epithelial tight junction barrier is mediated by NF-κB activation. PLoS ONE. https://doi.org/10.1371/journal.pone.0249544

Al-Sadi R, Ye D, Dokladny K, Ma TY (2011) Author manuscript; available in PMC

Altschul SF, Gish W, Miller W et al (1990) Basic local alignment search tool. J Mol Biol 215:403–410. https://doi.org/10.1016/S0022-2836(05)80360-2

Anandhakrishnan A, Korbonits M (2016) Glucagon-like peptide 1 in the pathophysiology and pharmacotherapy of clinical obesity. World J Diabetes 7:572. https://doi.org/10.4239/wjd.v7.i20.572

Ang Z, Ding JL (2016) GPR41 and GPR43 in obesity and inflammation—protective or causative? Front Immunol 7

Aslam M, Ladilov Y (2022) Emerging role of cAMP/AMPK signaling. Cells 11

Baldini G, Phelan KD (2019) The melanocortin pathway and control of appetite-progress and therapeutic implications. J Endocrinol 241:R1–R33. https://doi.org/10.1530/JOE-18-0596

Bliesner A, Eccles-Smith J, Bates C et al (2022) Impact of food-based weight loss interventions on gut microbiome in individuals with obesity: a systematic review. Nutrients 14:1–18. https://doi.org/10.3390/nu14091953

Caporaso JG, Lauber CL, Walters WA et al (2012) Ultra-high-throughput microbial community analysis on the Illumina HiSeq and MiSeq platforms. ISME J 6:1621–1624. https://doi.org/10.1038/ismej.2012.8

Chao AM, Tronieri JS, Amaro A, Wadden TA (2023) Semaglutide for the treatment of obesity. Trends Cardiovasc Med 33:159–166

Chen J, Mei A, Wei Y et al (2022) GLP-1 receptor agonist as a modulator of innate immunity. Front Immunol 13:1–9. https://doi.org/10.3389/fimmu.2022.997578

Chen XY, Chen L, Yang W, Xie AM (2021) GLP-1 suppresses feeding behaviors and modulates neuronal electrophysiological properties in multiple brain regions. Front Mol Neurosci 14

Christoff AP, Fernanda A, Sereia R et al (2017) Sequencing neoprospecta microbiome technologies bacterial identification through accurate library preparation and high-throughput sequencing. White Paper: Bacterial NGS

Clemente JC, Ursell LK, Parfrey LW, Knight R (2012) The impact of the gut microbiota on human health: an integrative view. Cell 148:1258–1270

Cryan JF, O'Riordan KJ, Cowan CSM et al (2019) The microbiota-gut-brain axis. Physiol Rev 99:1877–2013. https://doi.org/10.1152/physrev.00018.2018.-The

De La Serre CB, Ellis CL, Lee J et al (2010) Propensity to high-fat diet-induced obesity in rats is associated with changes in the gut microbiota and gut inflammation. Am J Physiol Gastrointest Liver Physiol 299:440–448. https://doi.org/10.1152/ajpgi.00098.2010

Derghal A, Astier J, Sicard F et al (2019) Leptin modulates the expression of mirnas-targeting POMC mRNA by the JAK2-STAT3 and PI3K-akt pathways. J Clin Med. https://doi.org/10.3390/jcm8122213

Drucker DJ (2022) GLP-1 physiology informs the pharmacotherapy of obesity. Mol Metab 57:101351. https://doi.org/10.1016/j.molmet.2021.101351

Du S, Zheng H (2021a) Role of FoxO transcription factors in aging and age-related metabolic and neurodegenerative diseases. Cell Biosci 11

Du S, Zheng H (2021b) Role of FoxO transcription factors in aging and age-related metabolic and neurodegenerative diseases. Cell Biosci 11

Duan X, Zhang L, Liao Y et al (2024) Semaglutide alleviates gut microbiota dysbiosis induced by a high-fat diet. Eur J Pharmacol 969:176440. https://doi.org/10.1016/J.EJPHAR.2024.176440

Fiebich BL, Batista CRA, Saliba SW et al (2018) Role of microglia TLRs in neurodegeneration. Front Cell Neurosci. https://doi.org/10.3389/fncel.2018.00329

Fock E, Parnova R (2023) Mechanisms of blood–brain barrier protection by microbiota-derived short-chain fatty acids. Cells 12

Fonseca VA, Zinman B, Nauck MA, et al (2010) Confronting the Type 2 diabetes epidemic: the emerging role of incretin-based therapies. Am J Med 123

Frost G, Sleeth ML, Sahuri-Arisoylu M et al (2014) The short-chain fatty acid acetate reduces appetite via a central homeostatic mechanism. Nat Commun 5:1–11. https://doi.org/10.1038/ncomms4611

Gabery S, Salinas CG, Paulsen SJ et al (2020a) Semaglutide lowers body weight in rodents via distributed neural pathways. JCI Insight. https://doi.org/10.1172/jci.insight.133429

Grasset E, Puel A, Charpentier J et al (2017) A specific gut microbiota dysbiosis of Type 2 diabetic mice induces GLP-1 resistance through an enteric NO-dependent and gut-brain axis mechanism. Cell Metab 25:1075-1090.e5. https://doi.org/10.1016/j.cmet.2017.04.013

Hasan N, Yang H (2019) Factors affecting the composition of the gut microbiota, and its modulation. PeerJ 2019

Hernández MAG, Canfora EE, Jocken JWE, Blaak EE (2019) The short-chain fatty acid acetate in body weight control and insulin sensitivity. Nutrients 11

Hill MO (1973) Diversity and evenness: a unifying notation and its consequences Author (s): M. O. Hill Published by: Ecological Society of America DIVERSITY AND EVENNESS: A UNIFYING NOTATION AND ITS CONSEQUENCES '. Ecology 54:427–432

Holst JJ, Andersen DB, Grunddal KV (2022) Actions of glucagon-like peptide-1 receptor ligands in the gut. Br J Pharmacol 179:727–742. https://doi.org/10.1111/bph.15611

Hong YH, Nishimura Y, Hishikawa D et al (2005) Acetate and propionate short chain fatty acids stimulate adipogenesis via GPCR43. Endocrinology 146:5092–5099. https://doi.org/10.1210/en.2005-0545

Hupa-Breier KL, Dywicki J, Hartleben B et al (2021) Dulaglutide alone and in combination with empagliflozin attenuate inflammatory pathways and microbiome dysbiosis in a non-diabetic mouse model of nash. Biomedicines. https://doi.org/10.3390/biomedicines9040353

Jais A, Brüning JC (2017) Hypothalamic inflammation in obesity and metabolic disease. J Clin Investig 127:24–32. https://doi.org/10.1172/JCI88878

Jandhyala SM, Talukdar R, Subramanyam C et al (2015) Role of the normal gut microbiota. World J Gastroenterol 21:8836–8847. https://doi.org/10.3748/wjg.v21.i29.8787

Jones ES, Nunn N, Chambers AP et al (2019) Modified peptide YY molecule attenuates the activity of NPY/AgRP neurons and reduces food intake in male mice. Endocrinology (United States) 160:2737–2747. https://doi.org/10.1210/en.2019-00100

Kahn BB, Alquier T, Carling D, Hardie DG (2005) AMP-activated protein kinase: ancient energy gauge provides clues to modern understanding of metabolism. Cell Metab 1:15–25

Kant R, Chandra L, Verma V et al (2022) Gut microbiota interactions with anti-diabetic medications and pathogenesis of type 2 diabetes mellitus. World J Methodol 12:246–257. https://doi.org/10.5662/wjm.v12.i4.246

Karmi A, Iozzo P, Viljanen A et al (2010) Increased brain fatty acid uptake in metabolic syndrome. Diabetes 59:2171–2177. https://doi.org/10.2337/db09-0138

Kim MS, Pak YK, Jang PG et al (2006) Role of hypothalamic Foxo1 in the regulation of food intake and energy homeostasis. Nat Neurosci 9:901–906. https://doi.org/10.1038/nn1731

Kimura I, Ozawa K, Inoue D et al (2013) The gut microbiota suppresses insulin-mediated fat accumulation via the short-chain

fatty acid receptor GPR43. Nat Commun. https://doi.org/10.1038/ncomms2852
Kimura I, Inoue D, Hirano K, Tsujimoto G (2014) The SCFA receptor GPR43 and energy metabolism. Front Endocrinol (Lausanne) 5
Kodani N, Nakae J (2020) Tissue-specific metabolic regulation of FOXO-binding protein: FOXO does not act alone. Cells 9
Lee DM, Battson ML, Jarrell DK et al (2018) SGLT2 inhibition via dapagliflozin improves generalized vascular dysfunction and alters the gut microbiota in type 2 diabetic mice. Cardiovasc Diabetol. https://doi.org/10.1186/s12933-018-0708-x
Lexchin J, Mintzes B (2023) Semaglutide: a new drug for the treatment of obesity. Drug Ther Bull 61:182–188. https://doi.org/10.1136/DTB.2023.000007
Li Y, Jiang Q, Wang L (2021) Appetite regulation of TLR4-induced inflammatory signaling. Front Endocrinol (Lausanne) 12
Liu X, Zheng H (2021) Modulation of sirt1 and foxo1 on hypothalamic leptin-mediated sympathetic activation and inflammation in diet-induced obese rats. J Am Heart Assoc. https://doi.org/10.1161/JAHA.120.020667
Liu L, Liu H, Fu C et al (2017) Acetate induces anorexia via up-regulating the hypothalamic pro-opiomelanocortin (POMC) gene expression in rabbits. J Anim Feed Sci 26:266–273. https://doi.org/10.22358/jafs/75979/2017
Loh M, Zhou L, Ng HK, Chambers JC (2019) Epigenetic disturbances in obesity and diabetes: epidemiological and functional insights. Mol Metab 27:S33–S41
Madsen MSA, Holm JB, Pallejà A et al (2019) Metabolic and gut microbiome changes following GLP-1 or dual GLP-1/GLP-2 receptor agonist treatment in diet-induced obese mice. Sci Rep 9:1–12. https://doi.org/10.1038/s41598-019-52103-x
Mao T, Zhang C, Yang S et al (2024) Semaglutide alters gut microbiota and improves NAFLD in db/db mice. Biochem Biophys Res Commun 710:149882. https://doi.org/10.1016/j.bbrc.2024.149882
Martin TL, Alquier T, Asakura K et al (2006) Diet-induced obesity alters AMP kinase activity in hypothalamus and skeletal muscle. J Biol Chem 281:18933–18941. https://doi.org/10.1074/jbc.M512831200
Martins FF, Santos-Reis T, Marinho TS et al (2023) Hypothalamic anorexigenic signaling pathways (leptin, amylin, and proopiomelanocortin) are semaglutide (GLP-1 analog) targets in obesity control in mice. Life Sci. https://doi.org/10.1016/j.lfs.2022.121268
Maslowski KM, Vieira AT, Ng A et al (2009) Regulation of inflammatory responses by gut microbiota and chemoattractant receptor GPR43. Nature 461:1282–1286. https://doi.org/10.1038/nature08530
May AT, Crowe MS, Blakeney BA et al (2019) Identification of expression and function of the glucagon-like peptide-1 receptor in colonic smooth muscle. Peptides (NY) 112:48–55. https://doi.org/10.1016/j.peptides.2018.11.007
Montandon SA, Jornayvaz FR (2017) Effects of antidiabetic drugs on gut microbiota composition. Genes (Basel). https://doi.org/10.3390/genes8100250
Morrow NM, Morissette A, Mulvihill EE (2024) Immunomodulation and inflammation: role of GLP-1R and GIPR expressing cells within the gut. Peptides (NY) 176:171200. https://doi.org/10.1016/j.peptides.2024.171200
Morton GJ, Cummings DE, Baskin DG et al (2006) Central nervous system control of food intake and body weight. Nature 443:289–295
Müller TD, Finan B, Bloom SR et al (2019) Glucagon-like peptide 1 (GLP-1). Mol Metab 30:72–130
Nasrin N, Kaushik VK, Fortier E et al (2009) JNK1 phosphorylates SIRT1 and promotes its enzymatic activity. PLoS ONE 4:8414. https://doi.org/10.1371/journal.pone.0008414
Naznin F, Toshinai K, Waise TMZ et al (2015) Diet-induced obesity causes peripheral and central ghrelin resistance by promoting inflammation. J Endocrinol 226:81–92. https://doi.org/10.1530/JOE-15-0139
Nogueiras R, Habegger KM, Chaudhary N et al (2012) Sirtuin 1 and sirtuin 3: physiological modulators of metabolism. Physiol Rev 92:1479–1514. https://doi.org/10.1152/physrev.00022.2011
Obadia N, Andrade G, Leardini-Tristão M et al (2022) TLR4 mutation protects neurovascular function and cognitive decline in high-fat diet-fed mice. J Neuroinflammation. https://doi.org/10.1186/s12974-022-02465-3
Perdomo CM, Cohen RV, Sumithran P et al (2023) Contemporary medical, device, and surgical therapies for obesity in adults. The Lancet 401:1116–1130
Qin Y, Havulinna AS, Liu Y et al (2022) Combined effects of host genetics and diet on human gut microbiota and incident disease in a single population cohort. Nat Genet 54:134–142. https://doi.org/10.1038/s41588-021-00991-z
Razazan A, Karunakar P, Mishra SP et al (2021) Activation of microbiota sensing – free fatty acid receptor 2 signaling ameliorates amyloid-β induced neurotoxicity by modulating proteolysis-senescence axis. Front Aging Neurosci. https://doi.org/10.3389/fnagi.2021.735933
Richards P, Thornberry NA, Pinto S (2021) The gut–brain axis: identifying new therapeutic approaches for type 2 diabetes, obesity, and related disorders. Mol Metab 46
Robinson A, Lubitz I, Atrakchi-Baranes D et al (2019) Combination of insulin with a GLP1 agonist is associated with better memory and normal expression of insulin receptor pathway genes in a mouse model of Alzheimer's disease. J Mol Neurosci 67:504–510. https://doi.org/10.1007/s12031-019-1257-9
Romanatto T, Cesquini M, Amaral ME et al (2007) TNF-α acts in the hypothalamus inhibiting food intake and increasing the respiratory quotient-effects on leptin and insulin signaling pathways. Peptides (NY) 28:1050–1058. https://doi.org/10.1016/j.peptides.2007.03.006
Rosario W, D'Alessio D (2015) An innate disposition for a healthier gut: Glp-1r signaling in intestinal epithelial lymphocytes. Diabetes 64:2329–2331. https://doi.org/10.2337/db15-0436
Secher A, Jelsing J, Baquero AF et al (2014) The arcuate nucleus mediates GLP-1 receptor agonist liraglutide-dependent weight loss. J Clin Investig 124:4473–4488. https://doi.org/10.1172/JCI75276
Shang J, Liu F, Zhang B et al (2021) Liraglutide-induced structural modulation of the gut microbiota in patients with type 2 diabetes mellitus. PeerJ 9:1–19. https://doi.org/10.7717/peerj.11128
Silva YP, Bernardi A, Frozza RL (2020b) The role of short-chain fatty acids from gut microbiota in gut-brain communication. Front Endocrinol (Lausanne) 11:1–14. https://doi.org/10.3389/fendo.2020.00025
Silva YP, Bernardi A, Frozza RL (2020a) The role of short-chain fatty acids from gut microbiota in gut-brain communication. Front Endocrinol (Lausanne) 11
Sina C, Gavrilova O, Förster M et al (2009) G Protein-coupled receptor 43 is essential for neutrophil recruitment during intestinal inflammation. J Immunol 183:7514–7522. https://doi.org/10.4049/jimmunol.0900063
Singh G, Krauthamer M, Bjalme-Evans M (2022a) Wegovy (Semaglutide): a new weight loss drug for chronic weight management. J Investig Med 70:5–13
Singh I, Wang L, Xia B et al (2022b) Activation of arcuate nucleus glucagon-like peptide-1 receptor-expressing neurons suppresses food intake. Cell Biosci. https://doi.org/10.1186/s13578-022-00914-3
Sohn JW (2015) Network of hypothalamic neurons that control appetite. BMB Rep 48:229–233. https://doi.org/10.5483/BMBRep.2015.48.4.272

Song Q, Zhang X (2022) The role of gut–liver axis in gut microbiome dysbiosis associated NAFLD and NAFLD-HCC. Biomedicines 10

Sonnenburg JL, Bäckhed F (2016) Diet-microbiota interactions as moderators of human metabolism. Nature 535:56–64

Sun H, Shu J, Tang J et al (2024) GLP-1 receptor agonists alleviate colonic inflammation by modulating intestinal microbiota and the function of group 3 innate lymphoid cells. Immunology 172:451–468. https://doi.org/10.1111/imm.13784

Susanti VY, Sasaki T, Yokota-Hashimoto H et al (2014) Sirt1 rescues the obesity induced by insulin-resistant constitutively-nuclear FoxO1 in POMC neurons of male mice. Obesity 22:2115–2119. https://doi.org/10.1002/oby.20838

Thaler JP, Yi CX, Schur EA et al (2012) Obesity is associated with hypothalamic injury in rodents and humans. J Clin Investig 122:153–162. https://doi.org/10.1172/JCI59660

Tsaousidou E, Paeger L, Belgardt BF et al (2014) Distinct roles for JNK and IKK activation in agouti-related peptide neurons in the development of obesity and insulin resistance. Cell Rep 9:1495–1506. https://doi.org/10.1016/j.celrep.2014.10.045

Valdearcos M, Robblee MM, Benjamin DI et al (2014) Microglia dictate the impact of saturated fat consumption on hypothalamic inflammation and neuronal function. Cell Rep 9:2124–2138. https://doi.org/10.1016/j.celrep.2014.11.018

Wang Y, Qian PY (2009) Conservative fragments in bacterial 16S rRNA genes and primer design for 16S ribosomal DNA amplicons in metagenomic studies. PLoS ONE. https://doi.org/10.1371/journal.pone.0007401

Wang L, Li P, Tang Z et al (2016) Structural modulation of the gut microbiota and the relationship with body weight: compared evaluation of liraglutide and saxagliptin treatment. Sci Rep. https://doi.org/10.1038/srep33251

Wang Z, Saha S, Van Horn S et al (2017) Gut microbiome differences between metformin- and liraglutide-treated T2DM subjects. Endocrinol Diabetes Metab. https://doi.org/10.1002/EDM2.9

Wang Z, Saha S, Van Horn S et al (2018) Gut microbiome differences between metformin- and liraglutide-treated T2 DM subjects. Endocrinol Diabetes Metab. https://doi.org/10.1002/edm2.9

Wilding JPH, Batterham RL, Calanna S et al (2021) Once-weekly semaglutide in adults with overweight or obesity. N Engl J Med 384:989–1002. https://doi.org/10.1056/nejmoa2032183

Wong CK, Yusta B, Koehler JA et al (2022) Divergent roles for the gut intraepithelial lymphocyte GLP-1R in control of metabolism, microbiota, and T cell-induced inflammation. Cell Metab 34:1514-1531.e7. https://doi.org/10.1016/j.cmet.2022.08.003

Wu H, Esteve E, Tremaroli V et al (2017) Metformin alters the gut microbiome of individuals with treatment-naive type 2 diabetes, contributing to the therapeutic effects of the drug. Nat Med 23:850–858. https://doi.org/10.1038/nm.4345

Xiao S, Zhang Z, Chen M et al (2019) Xiexin Tang ameliorates dyslipidemia in high-fat diet-induced obese rats via elevating gut microbiota-derived short chain fatty acids production and adjusting energy metabolism. J Ethnopharmacol 241:112032. https://doi.org/10.1016/J.JEP.2019.112032

Xiao S, Jiang S, Qian D, Duan J (2020) Modulation of microbially derived short-chain fatty acids on intestinal homeostasis, metabolism, and neuropsychiatric disorder. Appl Microbiol Biotechnol 104:589–601

Xu J, Jackson CW, Khoury N et al (2018) Brain SIRT1 mediates metabolic homeostasis and neuroprotection. Front Endocrinol (Lausanne) 9

Yang G, Chen S, Deng B, et al (2018) Implication of G protein-coupled receptor 43 in intestinal inflammation: a mini-review. Front Immunol 9

Yusta B, Baggio LL, Koehler J et al (2015) GLP-1R agonists modulate enteric immune responses through the intestinal intraepithelial lymphocyte GLP-1R. Diabetes 64:2537–2549. https://doi.org/10.2337/db14-1577

Zhang X, Zhang G, Zhang H et al (2008) Hypothalamic IKKβ/NF-κB and ER stress link overnutrition to energy imbalance and obesity. Cell 135:61–73. https://doi.org/10.1016/j.cell.2008.07.043

Zhao L, Chen Y, Xia F et al (2018) A glucagon-like peptide-1 receptor agonist lowers weight by modulating the structure of gut microbiota. Front Endocrinol (Lausanne) 9:1–13. https://doi.org/10.3389/fendo.2018.00233